2009년 2월
박사학위논문

The study of the P3 on the neuroprotective effect against DNA damage

조선대학교 대학원

의학과

김 승 곤

The study of the P3 on the neuroprotective effect against DNA damage

신경세포 DNA손상 보호작용을 지닌 P3 연구

2009년 2월 일

조선대학교 대학원

의학과

김 승 곤

The study of the P3 on the neuroprotective effect against DNA damage

지도교수 김 학 렬

이 논문을 의학박사 학위신청논문으로 제출함.

2008 년 10 월 일

조선대학교 대학원

의학과

김 승 곤

김 승 곤의 박사학위논문을 인준함

위원장 조선 대학교 교 수 박 상 학 인

위 원 조선 대학교 교 수 김 상 훈 인

위 원 조선 대학교 교 수 유 호 진 인

위 원 조선 대학교 조교수 황 걸 인

위 원 조선 대학교 교 수 김 학 렬 인

2008 년 12 월 일

조선대학교 대학원

CONTENTS

III. RESULTS

LIST OF FIGURES

ABSTRACT

The study of the P3 on the neuroprotective effect against DNA damage

Kim Seung-Gon
Advisor : Prof. Kim Hack Ryul M.D.,Ph.D.
Department of Medicine, Graduate School of
Chosun University

P3 is initially identified as a p53 downstream target involved in the ROS generation. Here we report that knockdown of P3 sensitizes cells to UV and radiomimetic drugs, impaired DNA repair, and defects both in intra-S-phase and G2/M checkpoints in response to DNA damage. P3 formed DNA damage-induced nuclear foci that is phosphatidylinositol 3-kinase-like family of serine/threonine protein kinases (PIKKs) dependent. Notably, P3 and γ-H2AX coimmunoprecipitate and colocalization in DNA damage foci, and efficient induction and maintenance of H2AX phosphorylation after DNA damage is impaired in P3 knockdown cells. Following DNA damage, P3 colocalized and associated with several DNA damage sensors and mediators, and contribute to the recruitment of these elements on the sites of DNA break lesions. Importantly, early cellular response to DNA damage is suppressed in p53-deficient

cells, and expression of P3 in a p53-deficient cells restores γ-H2AX signals as well as the recruitment of 53BP1 and Mre11 at DNA breaks, whereas, in p53 gain of function mutant cells, these response is not affected by P3. Our results suggest that P3 contributes to upstream induction of DNA damage signal, depending on the p53 status of the cells, and is an essential for p53-mediated triggering the appropriate early DNA damage response.

INTRODUCTION

The DNA damage response is a complex signaling process involving the orchestration of a variety of cellular events that rapidly activate in response to DNA damage. This signaling process involves a number of factors to either arrest the cell cycle and facilitate DNA repair (called the DNA damage checkpoint) or, if the DNA damage is too extensive to be repaired, induce apoptosis (1-4). The members of phosphatidylinositol 3-kinase-like kinases (PIKKs), ataxia telangiectasia mutated (ATM), ATM and Rad3 related (ATR), and DNA-dependent protein kinase (DNA-PK), become activated following DNA damage and transduce signals to downstream targets, including p53 and the checkpoint effector kinase Chk2 and Chk1 (5-9). The DNA damage response is considered to be a linear progression beginning with sensors that convey the initial damage signal to mediators and transducers, which in turn transmit the signal to numerous effectors. Dysfunction of the DNA damage response pathways in human cells leads to genomic instability and an increased risk of cancer progression (10, 11). Therefore, it is important to understand these complex mechanisms at the molecular level to further our knowledge of cancer progression and treatment. During the past few years, many studied have been conducted on how damage signals coordinately execute cellular responses to DNA damage; however, much less is known about the mechanisms that initiate the early events prompted by DNA damage that precede the spread of the damage signal throughout the cell.

The p53 tumor suppressor has been described as a “guardian of the genome” because of its critical role in coordinating cellular responses to genotoxic stress, including cell cycle arrest, DNA repair and apoptosis (12, 13). p53 is constitutely expressed at low levels but undergoes a significant increase in protein stability and

activity after DNA damage (14, 15). These events are thought to depend mainly on posttranslational modification that include phosphorylation by ATM/ATR, Chk1, and Chk2 kinases (9, 16-18). In cells derived from ataxia telangiectasia individuals, in which ATM is missing or inactivated, the DNA damage pathway and p53 response is abnormal (5, 19). Similarity, in some Li-Fraumeni patients with a defective Chk2, the p53 response is also compromised (20).

A major consequence of p53 activation following DNA damage is the induction of cell-cycle arrest at the G1/S or G2/M transition stages. This is achieved primarily through p53-induced expression of target genes that encode factors such as p21 that induces G1/S arrest (21), and proteins such as GADD45 and 14-3-3σ that are needed for an efficient G2/M arrest following DNA damage (22). Although a number of transcriptional targets of p53 have been identified, p53 effector functions remain incomplete (23). For example, even though p21 clearly participates in the G1 checkpoint responses, p21-/- mouse embryonic fibroblasts are only partially deficient in the G1 arrest elicited by p53, suggesting the existence of additional p53-dependent targets involved in cell-cycle regulation (24, 25). Furthermore, given that cells deficient for p53 apoptotic target genes typically display only partially compromised apoptosis (26), it is probable that there remain to be identified other mediators critical for p53-dependent apoptosis. Thus, there are likely to be additional, unidentified function of p53-inducible genes involved in mediating these different p53 responses.

P3 was originally identified through a serial analysis of gene expression study designed to identify genes induced by p53 before the onset of apoptosis (27). p53 interacts with a pentanucleotide microsatellite sequence within the P3 promoter $(TGYCC)_n$(Y=C or T), which is required for transcriptional activation of the P3 promoter by p53 (28). Analysis of the amino-acid sequence for P3 indicates

significant amino-acid homology with NADH quinine oxidoreductase 1 (NQO1) and suggests that, like NQO1, P3 is contributed to the generation of reactive oxygen species (ROS) (27), which are important downstream mediators of the p53-dependent apoptotic response. Moreover, human cellular apoptosis susceptibility protein (hCAS/CSE1L) interacts with P3 promoter and affects p53-dependent apoptosis by regulating P3 expression (29). However, because P3 expression alone is insufficient to induce apoptosis, it is assumed that several factors cooperate to cause apoptotic cell death (27). On the other hand, UV irradiation induce alternative splicing of P3 pre-mRNA to produce a splice variant protein, which is rapidly degraded by the proteasome degradation pathway, implicate the splicing machinery as a component of the cellular response to DNA damage (30). Therefore, the possibility may exist that P3 mediates unknown functions via cooperation of DNA damage response pathway. Here we show that P3 colocalized with several DNA damage sensors and early mediators upon DNA damage and is required for foci formation and phosphorylation of these molecules in ATM/ATR pathway. Furthermore, P3 is required for p53-mediated early DNA damage response, as demonstrated by induction of initial γ-H2AX signals and recruitment of DNA damage sensors and mediators at DNA lesions. Thus, we proposed that P3 functions as an upstream component of the DNA damage pathways that are critical for the activation and maintenance of DNA damage checkpoint signaling pathway and DNA repair.

MATERIALS AND METHODS

1. Cell culture and treatment

Neuro2A p53+/+ and p53-/- neuroblastome cells were cultured in Iscove's modified Dulbeco's medium (IMDM, Gibco-BRL, Grand island, NY) supplemented with 10% heat-inactivated fetal bovine serum (Camblex, Walkersville, MD), 100units/ml penicillin and 100 μg/ml streptomycin sulfate (Invitrogen, Carlsbad, CA) in a 5% CO_2 humidified incubator at 37°C. HeLa cervix adenocarcinoma cells were maintained in Dulbecco's modified Eagle Medium (DMEM, Gibco-BRL) and U2OS osteosarcoma cells were grown in McCoy's 5A medium (Camblex). Saos-2 osteosarcoma cells and SW480 colon carcinoma cells were cultured in RPMI 1640 medium (Gibco-BRL). Radiomimic drug, Bleomycin (Sigma, St. Louis, MO) and Neocarzinostatin (Sigma) were added to fresh cell media final concentration of 5mU, and 500ng/ml, respectively. For UV treatment, cells were rinsed in culture media and exposed to 254nm UVC lamp (UVP; Model UVGL-25) in a minimal volume of serum free culture media at a dose of 10J. After exposure of UV, changed complete culture media followed by continued culture at 37°C. To induce other DNA damages, fresh cell growth media containing 0.5 μM doxorubicin, 10mM hydroxyurea, 1μM camptothecin, 100μM H2O2 and 32 μM cisplatin was added for appropriate times.

2. Small interfering RNAs (siRNA) and transfection

For knockdown of P3 expression, the target site of siRNA was chosen from the human tumor protein p53 inducible protein 3 (TP53I3, P3) mRNA sequence (Gene Bank accession number NM_004881), which was extracted from the NCBI Entrez nucleotide database. This target site was also searched with National Center for

Biotechnology Information BLAST to confirm the specificity only to the human P3. The sequences of the 21-nucleotide sense and antisense RNA are as follows : 5`-AAAUGUUCAGGCUGGAGACUAdTdT-3` and 5`-UAGUCUCCAGCCUGAACAUUUdT dT-3`. Negative control siRNA duplex was purchased from Bioneer. The sequences are follows : 5`-CCUACGCCAAUUUCGUdTdT-3` and 5`-ACGAAAUUGGUGGCGUAGGdT dT-3`. siRNA duplexes were transiently transfected into the cells using RNAimax according to the manufacturer's instructions (invitrogen). These siRNAs were prepared by a transcription-based methods using the Silencer siRNA construction kits according to manufacturer's instructions (Ambion, Austin, TX). Cells were transfected with the constructed siRNA expression plasmid based on pSilencer-hygro vector (Ambion), which includes a human U6 promoter and a hygromycin resistance gene, using LipofectAMINE 2000 (Invitrogen). For stably knockdown of P3, after transfection with *psilencer*-empty or -P3 vector, we selected several resistant colonies against 300 μg/ml hygromycin in the culture medium. ATM, ATR and DNA-PK siRNA duplex was purchased from Santa cruz biotechnology.

3. Transfection of plasmid

For manufacture of P3 expression vector, the entire coding region of human P3 cDNA was amplified by RT-PCR using the P3 oligo primer : sense 5`-ATGTTAG CCGTGCACTTTGACAA-3` and antisense 5`-TCACTGGGGCAGTTCCAGGAC-3` from human fibroblast GM00637 cells. The amplified P3 PCR products were inserted into a mammalian expression *pcDNA3.1* neo vector or *pcDNA3.1* zeo vector containing a CMV promoter and neomycin resistance gene or zeocin resistance gene, respectively (Invitrogen). P3 sequences and orientation were confirmed by automated

DNA sequencing. If required, we selected antibiotics resistant colonies after transfection. To produce $p53^{R248W}$ and $p53^{R273H}$ mutants, pcDNA-myc3-wtp53 (a gift from JH Jeong, National University of Seoul) was used as template DNA. Site directed mutagenesis of p53 was performed using Muta-Direct^{TM} Site-Directed Mutagenesis kits according to manufacturer's instructions (iNtRON Biotech, Seoul, Korea). The sequences of mutagenesis-primer are as follows : forward primer 5`-ATGGGCGG CATGAACTGGAGGCCCATCCTC-3` and reverse primer 5'-GAGGATGGGCCTCC AGTTCATGCCGCCCAT-3' for $p53^{R248W}$ construct, and forward primer 5'-AACAGCTTT GAGGTGCATGTTTGTGCCTGT-3` and reverse primer 5`-ACAGGCACAAACATGCA CCTCAAAGCTGTT-3' for $p53^{R273H}$ construct. Cells were transfected with appropriate plasmid using LipofectAMINE 2000 (Invitrogen) according to manufacturer's instructions.

4. Cell survival assay

After UV radiation or treatment of NCS or BLM, 5×10^2 cells were immediately seeded onto 60mm dish in triplicate and grown for 2-3 weeks at 37°C to allow colonies to form. Colonies were stained with 2% methylene blue / 50% ethanol and counted. The fraction of surviving cells was calculated as the ratio of the plating efficiencies of treated cells to untreated cells. The mean value ± SD. for three independent experiments was determined.

5. PFGE analysis of DSB repair

For determination of DSB rejoining, cells were exposed to UV at 10J. After various recovery times, cells were resuspended at 5×10^7 cells/mL in 1% CleanCut agarose solution and cast into an agarose plug. Solidified agarose plug lysed for overnight in

1% N-Lauroyl sarcosine, 100mM EDTA (pH8.0), 0.2% Sodium deoxycholate, and 1mg/ml proteinase K according to the instructions of the manufacturer (Roche Diagnostic corp., Indianapolis, IN). The plugs were washed in Washing buffer and CHEF gel electrophoresis is performed in CHEF DRII apparatus (Bio-Rad, Hercules, CA) in 0.5×TBE at 14°C with field strength of 1.7V/cm. Pulse times was increased from 50 to 200s for 31h and then from 200 to 600s for 31h followed by increased from 2000 to 2200s for 31h. The gel was stained with 0.5 μg/ml ethidium bromide. The fraction of DNA migrating from the plug into the lane (% DNA extracted) was measured using a UV transilluminator and image analysis using Scion image software (Scion corp.).

6. Comet assay

Cells were treated with UV, trypsinized and resuspended in PBS. Aliquots of the cell suspension (20 μl, 1×10^5 cells) were transferred to 1.5 mL tubes and then mixed with 200 μl low-melting agarose and distributed onto conventional microscope slides. The slides were precoated with normal melting agarose (0.5% in PBS) and dried at room temperature. The agarose had solidified at 4°C for 10 min. The slides were then immersed in lysis solution (2.5 mol/L NaCl, 100 mmol/L Na_2EDTA, 10 mmol/L Tris-HCl (pH 10), containing freshly added 1% Triton X-100 and 10% DMSO]) for 1 h at 4°C and

then placed into a horizontal electrophoresis apparatus filled with freshly made buffer (1 mmol/L Na_2EDTA, 300 mmol/L NaOH (pH >13)). Electrophoresis was run for 30 min at 300 mA. At the end of the electrophoresis, slides were washed with the 70% ethanol, stained with 30-50μl ethidium bromide (40 μg/ml) for 1h, and kept in a moist chamber in the dark at 4°C until analysis. Cells were analyzed 24h after staining at

×400 magnification using a fluorescence microscope (Zeiss, R.G.) equipped with a 50-W mercury lamp. The microscope images revealed circular shapes, indicating undamaged DNA, and comet-like shapes, indicating the DNA had migrated out from the head to form a tail (damaged DNA).The extension of each comet was analyzed using a computerized image analysis system (Komet5.5, Andor Technology) that provided a ‘‘tail moment,’’ which is defined as the product of DNA in the tail and the mean distance of its migration in the tail and considered to be the variable most directly related to DNA damage. Calculation of the extent of DNA damage, which was not homogeneous, was based on analysis of 20 to 40 randomly selected comets from each slide.

7. Immunoprecipitation assay and Western Blot analysis

The cells were lysed in RIPA buffer (50mM Tris-HCl, pH7.5, 150mM sodium chloride, 1% Nonidet P-40, 0.5% sodium deoxycholate, 0.1% sodium dodecy sulfate) or M-PER buffer (Mammalian Protein Extraction Reagent, Pierce, Rockford, IL) with protease inhibitor (Roche Diagnostic corp., Indianapolis, IN). Equal amounts of protein were separated by 6-15% SDS-PAGE followed by electrotransfer onto a polyvinylidene difluoride membrane (Millipore, Bedfore, MA). The membranes were blocked with TBS-t (10 mM Tris-HCl, pH 7.4, 150 mM NaCl)containing 5% non-fat milk for 1h and then incubated at room temperature with primary antibodies. Blots were washed four times for 15 min with 0.5% Tween 20-containing TBS-t and then incubated for 1h with peroxidase conjugated secondary antibodies (1:5000, Jackson immunoResearch Inc. West Grove, PA). The membranes were washed again four times and developed using an enhanced chemiluminesence detection system (ECL, Amersham Corp., Cardiff, UK). For immunoprecipitation assay, the RIPA extracts

were pre-cleared with protein A-agarose bead (Amersham Corp., Cardiff, UK), and then incubated at 4°C overnight with fresh protein A-bead in the presence of appropriate antibodies. The beads were washed five times in RIPA buffer without protease inhibitor, resuspended in SDS sample buffer, and boiled for 5 min. Samples were analyzed by Western blotting using the appropriate antibodies to detect protein expression.

8. Preparation of Subcellular fractions

Neuro2A cells were harvested, and lysed in cytosol extraction buffer (CEB, 10mM HEPES, pH7.5, 3mM $MgCl_2$, 14mM KCl, 5% glycerol, 1mM DTT) with protease inhibitor (Roche) for 10min in ice. For complete lysis, 0.2% NP-40 was added followed by vortexing for 10s. After centrifugation at 8,600g for 2 min, the supernatant (cytosolic extracts) was transferred to new tubes. The pellet was washed three times in CEB, and lysed in Nuclear extraction buffer (NEB, 10mM HEPES, pH7.5, 3mM $MgCl_2$, 400mM NaCl, 5% glycerol, 1mM DTT) with protease inhibitor for 30min at 4°C followed by centrifugation at 13,200rpm for 30 min. The supernatant is nuclear extracts.

9. Antibodies

Antibodies against of P3 used in this study are P3 H300 (Santa Cruz Biotechnology, Santa Cruz, CA), P3 C-20 (Santa cruz) and P3 Ab-1 (Calbiochem). P3 protein was detected by Western blotting (WB) with a rabbit polyclonal P3 H300 antibody at 1:1000 dilution and P3 foci was also detected by immunofluorescence staining (IF) using P3 H300 antibody at 1:50 dilution. γH2AX was detected by IF and WB with mouse monoclonal antibody, clone JBW301 (Upstate Biotechnology, Temecula, CA)

at 1:200 and 1:1000 dilution, respectively. H2AX antibody was purchased from Upstate. Following antibodies were used for immunofluorescence staining : anti-53BP1 polyclonal antibody (Santa cruz, 1:50), anti-Mre11 monoclonal antibody (BD Phamingen, San Jose, CA, 1:200), anti-Nbs1 polyclonal antibody (Cell Signaling Technology, Danvers, MA, 1:200), anti-Rad50 monoclonal antibody (BD Phamingen, 1:200), anti-ATM protein kinase pS1981 monoclonal antibody (Rockland, Immunochemicals Ins., Philadelphia, PA, 1:500) anti-DNA-PK polyclonal antibody (Santa cruz, 1:50), anti-ATR-p(S428) polyclonal antibody (Cell Signaling Technology, a:200) and anti-p53 DO-1 monoclonal antibody (Santa cruz, 1:50). Following antibodies were used for Western blot analysis : anti-ATM 5C2 mAb (1:500), anti-ATR N-19 pAb (1:300), anti-DNA-PKcs G4 mAb (1:500) anti-p53 DO-1 mAb (1:2000), anti-αTubulin TU-02 mAb (1:5000), anti-Cdc25A mAb (1:500), anti-myc mAb (1:1000) and anti-53BP1 pAb (1:500, Santa cruz) ; anti-Chk1 pAb (1:1000), anti-Chk1-p(S345) pAb (1:1000), anti-Chk2 pAb(1:1000), anti-Chk2-p(T68) pAb (1:1000), anti-p38 pAb (1:1000), anti-p38-p(T180/Y182) pAb and anti-p53-p(S15) pAb (1:1000, Cell Signaling Technology); anti-Rad50 mAb (1:750), anti-Mre11 mAb (1:1000) and anti-Nbs1 mAb (1:1000, BD Phamingen).

10. Immunofluorescence microscope

Cells cultured on coverslips coated with poly-L-lysine (Sigma) were treated UV, NCS or BLM followed by recovery for adequate times. Cells were then washed with PBS twice, fixed with 4% paraformaldehyde for 10 min and then permeabilized with 0.3% Triton X-100 for 10 min at room temperature. After permeabilization, coverslip were washed PBS three times and then blocked with 5% BSA in PBS for 1h. Cells were single or double immunostained with primary antibodies against various proteins for

overnight at 4°C. Cells were washed with PBS and then stained appropriate Alexa Fluor 488-(green, Molecular Probe), Alexa Fluor 594-(red, Molecular Probe) conjugated secondary antibodies. After washing, cells were mounted using Vectashield mounting medium with 4,6 diamidino-2-phenylindole (Vector Laboratories, Burlingame, CA). Fluorescence images were taken using Zeiss Axioplan 2 imaging epifluorescent microscope equipped with a charge-coupled device camera and ISIS software (MetaSystems, Altlussheim, Germany).

11. BrdU incorporation assay

To determine cell populations in the S phase, the incorporation of BrdU was monitored as a parameter for DNA synthesis according to the instructions of the manufacturer (Roche Diagnostic corp.). Mock- and sip3 cells were plated in 48-well plate and treated with indicated dose of NCS, BLM or UV. After 24h, 10 μM BrdU was added to the culture medium for 2 h at 37°C for incorporation into freshly synthesized DNA. Following fixation of the cells, cellular DNA was partially digested by nuclease treatment. A peroxidase-labeled antibody to BrdU and a peroxidase substrate were sequentially added to yield a colored reaction product, which is proportional to the level of BrdU incorporated into cellular DNA. Colored products were measured at microplate reader at 405nm with a reference wavelength at approx. 490nm. The relative DNA synthesis was calculated as the percentage of absorbance of cells treated with DNA damaging agents from the absorbance of control cells. The data are presented as the average ± SD value of representative triplicate experiments.

12. Cytotoxicity assay- MTT assay

To show the effect of P3 on DNA damage-induced SW480 cell death, 2-(4,5-

dimethyl-triazol -2-yl)-2,5-diphenyl tetrazolium bromide (MTT, Sigma) assay was performed. The control or P3 siRNA, and mock or P3 expression vector-transiently transfected SW480 cells were seeded at a density of 1×10^4/well in 96well plate and then treated with 20J UV (middle) or 5mU BLM (right). After indicated times 10 μl of MTT reagent was added to each well and incubated for 3h. MTT crystals were dissolved with isopropanol containing 0.04N HCl and absorbance at 570nm was measured. The relative cell survival was calculated as the percentage of absorbance of cells treated with DNA damaging agents from the absorbance of control cells. Assays were repeated at least three times independently, and the data are presented as the average ± SD value of representative triplicate experiments.

13. G2/M checkpoint analysis

HeLa-sihygro and HeLa-sip3 cells were treated with 100ng/ml nocodazole for 3h following addition of 200ng/ml NCS or 10J UV. After 24h, cells were harvested and washed with PBS and then fixed with 1% formaldehyde for 10min at 37°C. Cells were immediately chilled on ice for 1min and then cells were permeabilized with 90% methanol at -20°C overnight. Fixed cells were washed with PBS and blocked with incubation buffer (0.5% BSA in PBS) for 10 min. Cells were stained with anti-phospho-Histone H3(S10)-Alexa Fluor 647 conjugate antibody (Cell signaling Technology) at 1:10 dilution in incubation buffer for 1h in the dark at room temperature. Cells were washed and then resuspended in PBS containing 50 μg/ml propidium iodide. At least 10,000 cells were analyzed by fluorescent-activated cell sorting (FACSort, Becton Dickinson, San Jose, CA). Acquired data were analyzed by cell Quest Pro software. (Becton Dickinson).

14. Flow cytometry by Propidium Iodide staining

The trypsin-detached cells were collected and washed with cold PBS, followed by fixing in 70% cold-ethanol for 30min at 4°C. The cells were then stained with PBS containing 50 μg/ml propidium iodide. Fluorescence emitted from the PI-DNA complex in each cell nucleus was measured after laser excitation at 488nm with a flow cytometry (FACSort, Becton Dickinson). For measurement of cell death, the percentage of cells in sub-G1 population was calculated. Aggregates of cell debris at the origin of histogram were excluded from the sub G1 cells.

15. Dephosphorylation with λ-protein phosphoatase

The cells were lysed in RIPA buffer (50mM Tris-HCl, pH7.5, 150mM sodium chloride, 1% Nonidet P-40, 0.5% sodium deoxycholate, 0.1% sodium dodecy sulfate) with protease inhibitor (Roche Diagnostic corp., Indianapolis, IN). 100μg lysates were incubated with 400 units λ-protein phosphoatase (New England Biolabs, Ipswich, MA) in phosphatase buffer (50mM Tris, pH7.5, 0.1mM Na_2EDTA, 5mM dithiothreitol, 2mM $MnCl_2$) for 30 min at 30 °C.

RESULTS

1. P3 knockdown cells display increased sensitivity to DNA damage agents and DNA repair defective phenotype

To determine whether P3 is involved in the DNA damage-induced cell death, we created Neuro2A and HeLa cell lines containing a stably integrated P3-targeting small hairpin RNA (shRNA) expression vector that silenced P3 expression with high efficiency. we then examined these and scramble shRNA expressing cells for analyzing their response to DNA damaging reagents. Control and P3 knockdown HeLa and Neuro2A cells were treated with ultraviolet (UV) or radiomimetic drug bleomycin (BLM), clonogenic survival assay was performed. Although pig3 is known to play a role in p53-mediated proapoptotic signaling through ROS generation (27), interestingly and surprisingly, the P3 knockdown cells were significantly more sensitive to UV (Figure 1A) and BLM (Figure 1B) than were control cells. This increased sensitivity in P3 knockdown cells could be attributed to defect of DNA damage repair that is distinct from its ROS generation and proapoptotic role. To explore this possibility, we directly monitored the activity of UV-induced DNA repair in P3 knockdown cells using pulsed-field gel electrophoresis (PFGE). We observed that, following UV irradiation, the percentage of DSBs remaining more increased in P3 knockdown cells than control cells (Figure 1C). Control Neuro2A cells efficiently repaired the majority of DSBs, with ~20% of DNA breaks remain unrejoined up to 20 h. In contrast, P3-depleted Neuro2A cells show severe defects in DSB repair, with more than 50~60% of DSBs remain unrejoined. To further confirm that P3 knockdown impairs DNA repair, we used a alkali comet assay that detect single or double strand breaks in DNA of single cells. 24 hr after UV irradiation, tail movement

were analyzed in 30~50 single cells per sample. We found that control and P3-depeleted Neuro2A cells have comparable amounts of DNA damage after UV irradiation. However, DNA repair was almost complete by 24 hr in control cells, whereas comet tails were still visible in P3 knockdown cells (Figure 1D), indicating that P3 knockdown compromises the ability of cells to repair to DNA damage.

2. P3 knockdown results in defects at intra-S and G2/M DNA damage checkpoints.

Since induced DNA repair and DNA checkpoint activation are generally accepted as critical components of cell survival following exposure to DNA damage, we next investigated whether P3 is involved in the regulation of intra S-phase and G2/M checkpoints following DNA damage. The S-phase checkpoint has a critical role in preventing spontaneous replication-fork collapse and is responsible for inhibiting S-phase progression after DNA damage. We observed that NCS- and UV-treated control Neuro2A cells exhibited significant inhibition of DNA synthesis (Figure 1E). In contrast, P3 depleted cells did not efficiently activates the S-phase checkpoint, as demonstrated by only small amounts of DNA synthesis inhibition (Figure 1E), indicating that P3 contributes to the intra-S phase checkpoint.

We next examined whether P3 plays a role in the G2/M checkpoint. The G2/M checkpoint is activated to prevent cells with damaged DNA or incomplete DNA replication from undergoing mitosis. Cells that fail to activate an S-phase checkpoint should prevent movement into mitosis by activating the G2/M checkpoint. To examine the effects of P3 on the G2/M checkpoint, control and P3-depeleted Neuro2A cells were mock treated or exposed to NCS or UV, and then labeled with anti-phosphohistone (Ser10) antibody, a marker for cells in M phase. In one set of

experiments, the microtubule-disrupting agent, nocodazole was added 3 hr following UV or NCS, to stop the cell cycle at mitosis. In contrast to control cells, which arrested in G2, a significantly higher proportion of P3 knockdown cells entered mitosis (Figure 1F), indicating that P3 is also involved in the G2/M phase checkpoint in response to DNA damage.

To evaluate the molecular nature of the cell-cycle defects observed in P3 knockdown cells, we examined the phosphorylation status of checkpoint-regulated molecules required for cell cycle arrest in response to DNA damage. Chk1 and Chk2, and p53 are key regulators in the control of intra-S and G2/M checkpoints, and are ATM and ATR downstream targets. In control HeLa cells, Chk1 and Chk2 were phosphorylated on their ATM/ATR target residues, Ser317 and Thr68, respectively, after DNA damage. However, there was significantly reduced phosphorylation of Chk1, as well as Chk2, in P3-depleted HeLa cells treated with UV (Figure 1G) or NCS (Figure 1H). We also found that p53 phosphorylation on Ser15 was markedly inhibited in UV-irradiated P3 knockdown MCF7 and Neuro2A cells, compared with their control cells. Another indicator of a functional ATM/Chk2 cascade, phosphatase Cdc25A (31) was also failed to rapidly decline in P3 depleted HeLa cells following NCS treatment. Since p38 MAPK activity has been recently reported to be involved in the G2/M transition and S phase progression in U2OS and HeLa cells following UV exposure (32-34), we also examined the levels of p38 phosphorylation in control and P3-deficient cells exposed to UV. In control cells, p38 phosphorylation was detected as early as 6~12 hr after UV irradiation. In marked contrast, P3-depleted U2OS and HeLa cells showed significant suppression of p38 phosphorylation at any time point. Taken together, our results indicate that P3 plays an important role in mediating DNA damage checkpoint responses.

A

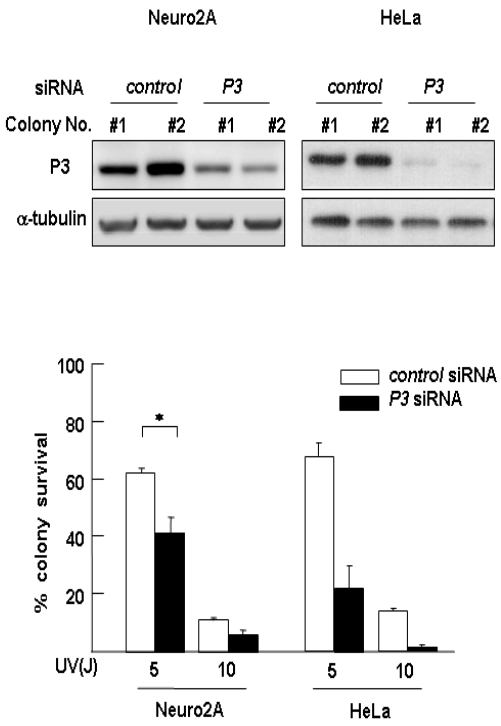
Neuro2A
HeLa
siRNA
control
P3
control
P3
Colony No.
#1
#2
#1
#2
#1
#2
#1
#2
P3
α-tubulin
100
80
60
40
20
% colony survival
control siRNA
P3 siRNA
*
UV(J)
5
10
5
10
Neuro2A
HeLa

B

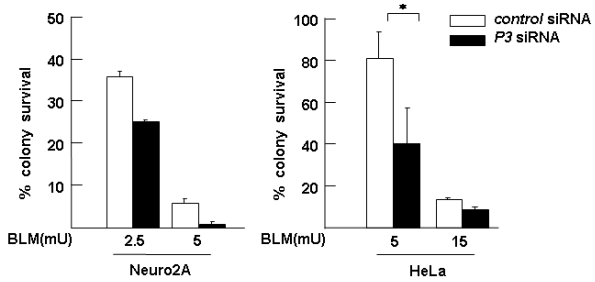
% colony survival
50
40
30
20
10
BLM(mU)
2.5
5
Neuro2A
100
80
60
40
20
BLM(mU)
5
15
HeLa
*
control siRNA
P3 siRNA

C

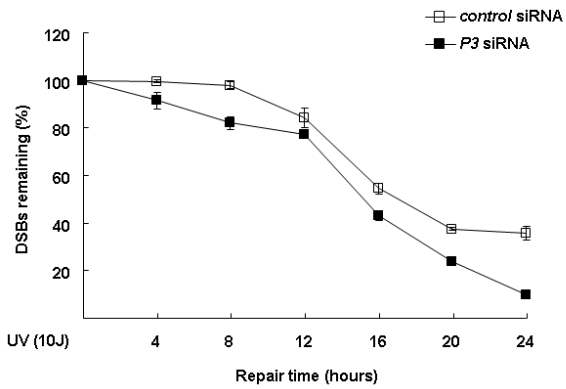
control siRNA
P3 siRNA
DSBs remaining (%)
120
100
80
60
40
20
UV (10J)
4
8
12
16
20
24
Repair time (hours)

D

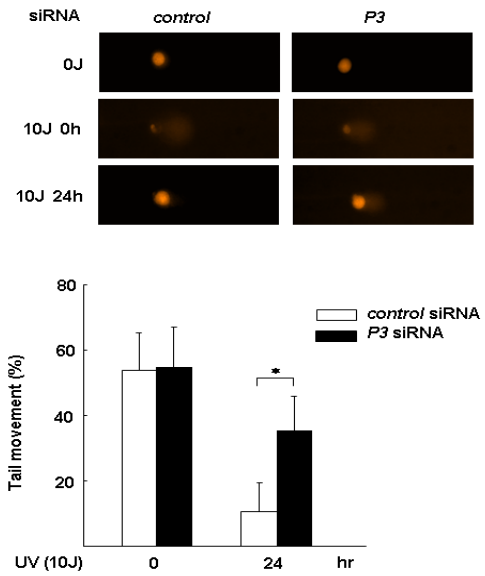
siRNA
control
P3
0J
10J 0h
10J 24h
80
60
40
20
Tail movement (%)
control siRNA
P3 siRNA
*
UV (10J)
0
24
hr

E

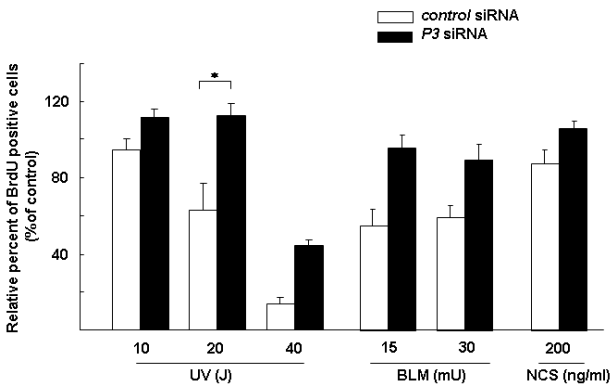
control siRNA
P3 siRNA
Relative percent of BrdU positive cells (%of control)
120
80
40
*
10
20
40
15
30
200
UV (J)
BLM (mU)
NCS (ng/ml)

F

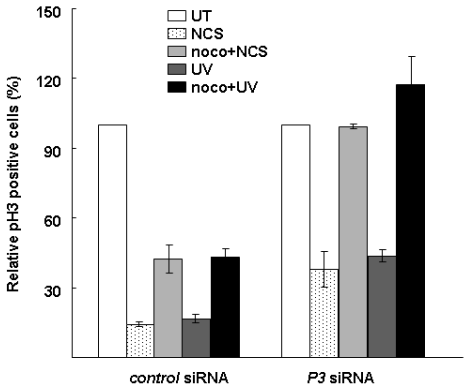
150
120
90
60
30
Relative pH3 positive cells (%)
UT
NCS
noco+NCS
UV
noco+UV
control siRNA
P3 siRNA

G

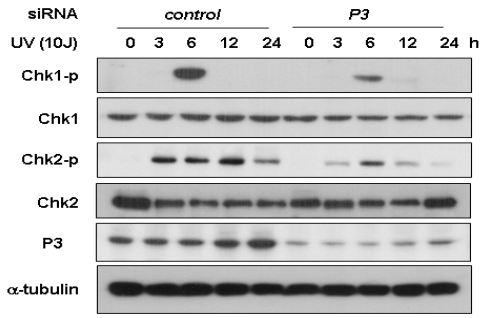
siRNA
control
P3
UV (10J)
0 3 6 12 24 0 3 6 12 24 h
Chk1-p
Chk1
Chk2-p
Chk2
P3
α-tubulin

H

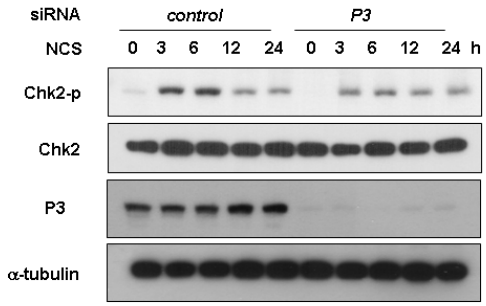
siRNA
control
P3
NCS
0 3 6 12 24 0 3 6 12 24 h
Chk2-p
Chk2
P3
α-tubulin

Figure 1. P3-deficient cells exhibit impaired DNA damage checkpoint activation.

(A and B) P3 knockdown sensitized Neuro2A and HeLa cells to UV (A) and BLM (B). Data are presented as mean ± standard deviation.

(C) PFGF analysis in indicated Neuro2A cells after UV (10 J/m^2). Data are presented as mean ± standard deviation.

(D) DNA damages of indicated Neuro2A cells induced by UV (10 J/m^2) were analyzed by single-cell gel electrophoresis. Data are presented as mean ± standard deviation.

(E) Neuro2A cells depleted of endogenous P3 were treated with indicated doses of UV or BLM, and the percentage of S-phase cells incorporating BrdU was determined. Data are presented as mean ± standard deviation.

(F) Indicated Neuro2A cells were untreated or treated with UV (10 J/m^2) or BLM (5 mU) in the presence or absence of nocodazole, and cells in mitosis were determined by staining with propidium iodide and phospho-histone H3 antibody. Data are presented as mean ± standard deviation.

(G and H) Indicated Neuro2A cells were treated with UV (10 J/m^2) (G) or NCS (200 ng/ml) (H), harvested at indicated times and then subjected to immunoblotting with indicated antibodies. Data are presented as mean ± standard deviation.

3. DNA damage-induced phosphorylation of H2AX is suppressed in P3-depleted cells

To address whether the lack of damage-induced checkpoints was the results of a defect in DNA damage sensor and mediator signaling pathway, we analyzed γ-H2AX signal in UV- or NCS-treated Neuro2A and HeLa cells. One of the earliest signal in the DNA damage response is phosphorylation of histone variant H2AX at Ser139. γ-H2AX is required for the sustained localization of a number of DNA-damage mediator/repair factors at or near the sites of DNA damage (35-38). Therefore, γ-H2AX plays an important role in initial recognition of DNA damage and recruiting DNA damage checkpoint proteins (36, 39). As shown in Figure 2A and 2B, after exposure to NCS or UV, H2AX phosphorylation rapidly increased within 1 h or 3 hr in control Neuro2A and HeLa cells, respectively, and reached the peak at the 3~6 h time point. However, in P3 knockdown cells, H2AX phosphorylation was significantly diminished after UV or NCS and failed to propagate.

We next investigated whether P3 would affect γ-H2AX foci formation after DNA damage by immunofluorescence assay. Consistent with the phosphorylation, P3 depleted cells exhibited significantly impaired γ-H2AX foci formation after UV and NCS treatment. In control cells, the γ-H2AX foci became bigger and brighter as early as about 30 min and 3 hr after NCS (Figure 2C) and UV (Figure 2D) treatment, respectively, and the number of γ-H2AX foci decreased 12-24 hr after NCS and UV treatment (data not shown). However, although γ-H2AX foci rapidly formed foci following NCS and UV in P3 knockdown cells, the intensity of γ-H2AX foci was significantly reduced in P3-depleted cells than those in control cells. The number of foci observed did not correspond to predicted DSBs. This is probably due to weaker γ-H2AX signals that were below the threshold of detection. Thus, these results suggest

that P3 has an important role in initiating or amplifying H2AX phosphorylation after DNA damage.

To address whether P3 also have the capacity to trigger H2AX phosphorylation in response to other type of genotoxic insult, control and P3-deficient Neuro2A cells were treated with doxorubicin (topoisomerase II inhibitor), hydroxyurea (ribonuclease reductase inhibitor), camptothecin (topoisomerase I inhibitor), H2O2 (single strand break inducer), and cisplatin (DNA cross-link agents), and analyzed cell lysates for γ-H2AX signals. As shown in Figure S6, H2AX phosphorylation was also significantly suppressed in P3-deficient Neuro2A cells.

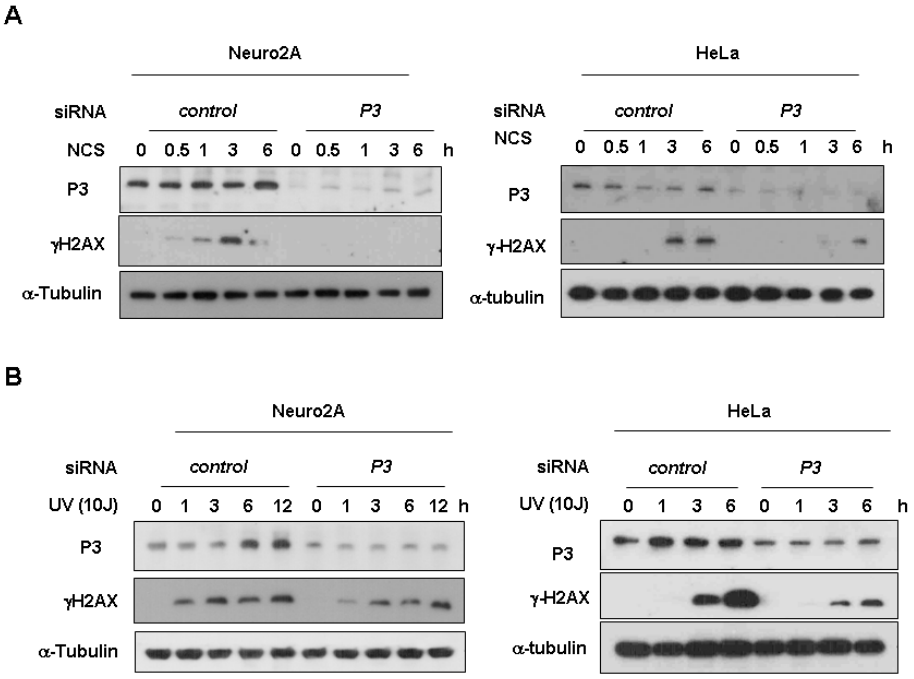
A
Neuro2A
HeLa
siRNA
control
P3
NCS
0 0.5 1 3 6 0 0.5 1 3 6 h
P3
γH2AX
α-Tubulin
α-tubulin
B
UV (10J)
0 1 3 6 12 0 1 3 6 12 h
0 1 3 6 0 1 3 6 h

C

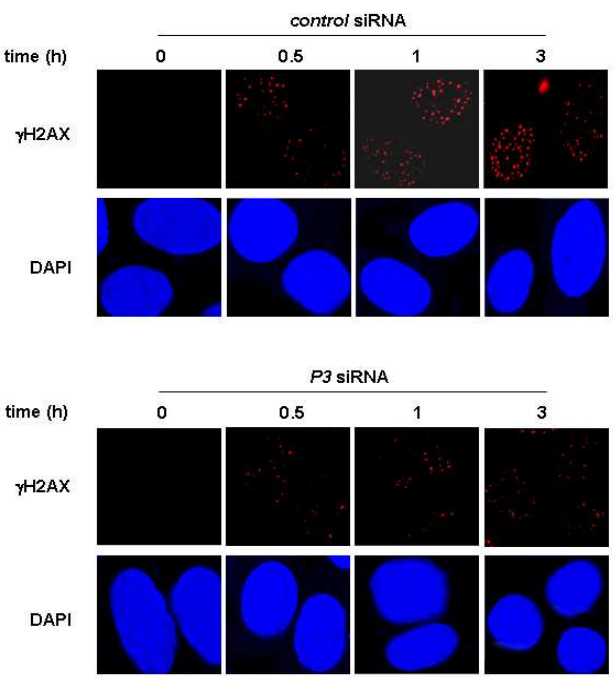
control siRNA
time (h)
0
0.5
1
3
γH2AX
DAPI
P3 siRNA
time (h)
0
0.5
1
3
γH2AX
DAPI

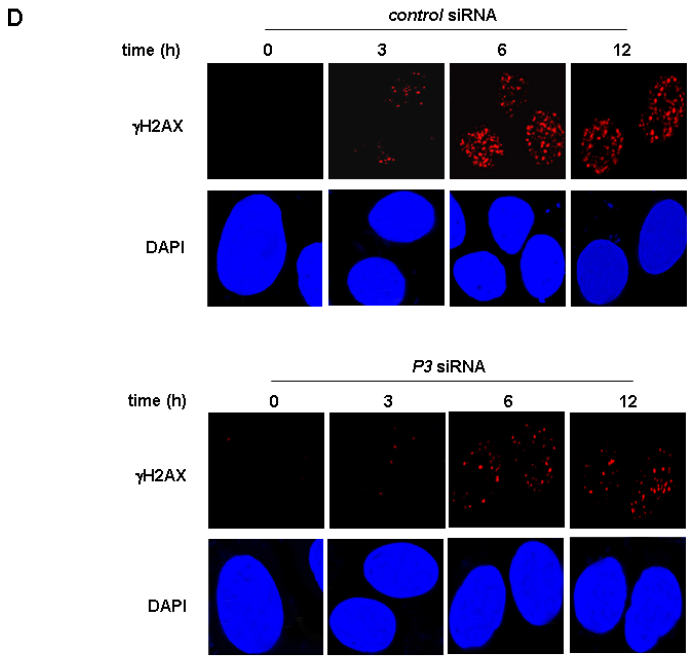

Figure 2. P3 knockdown impairs γ-H2AX signals in response to DNA damage

(A and B) H2AX phosphorylation analysis of P3-depleted HCT16 and HeLa cells. Time-course analysis of H2AX phosphorylation by Immunoblotting after 200 ng/ml of NCS (A) or 10 J/m^2 of UV (B).

(C and D) Control or P3-depleted Neuro2A cells were treated with 200 ng/ml of NCS (C) or 10 J/m^2 of UV (D) and immunostained with γ-H2AX antibody.

4. P3 forms nuclear foci and colocalizes with γ-H2AX in response to DNA damage.

Several DNA damage signaling proteins are targets for ATM/ATR-mediated phosphorylation and participate in transmitting the DNA damage signal to downstream targets. After DNA damage, those proteins are recruited to the sites of DNA damage and form discrete DNA damage-induced nuclear foci. The order and timing of these events are thought to be critical for checkpoint response and DNA repair (40). Thus, we were interested in knowing whether P3 is also formed UV- or NCS-induced nuclear foci.

Previous report showed that P3 was localized to the cytoplasm in H1299 cells expressing p53 (41). However, we observed that, although P3 mainly localized in cytosolic fraction, about 30% of total P3 was also present in nucleus. Moreover, we demonstrated that N-terminal region (1-460 nt) of P3 is essential for nuclear localization of P3, suggesting that P3 was located in both the nuclear and cytoplasm. Immunofluorescence staining indicated that P3 showed diffuse staining of nuclei in Neuro2A, HeLa, and MCF7 cells without UV or NCS. However, P3 formed nuclear foci promptly and the number of P3 foci promptly increased after NCS or UV treatment (Figure 3A). The induction of P3 foci by UV, NCS, or BLM raises the possibility that these foci represents actual sites of DNA breaks. In fact, we observed that the number of P3 foci was remarkable colocalization to that of γ-H2AX throughout the course of the experiment (Figure 3B). We also found that P3 and γ-H2AX physically interact after UV irradiation (Figure 3C), indicating that P3 very upstream of the DNA damage signaling. The ATM, ATR and DNA-PK participates in the foci formation of the MRN complex, γH2AX and 53BP1 (11, 42). Thus, we investigated whether P3 foci formation was PIKKs dependent. Treatment of wortmannin, inhibitors of the PIKKs, severely diminished P3 foci formation in

response to DNA damage (Figure 3D). We then examined P3 foci formation in HeLa cells deficient in ATM, ATR, or DNA-PK by transiently transfection of their specific siRNAs. ATM, ATR, or DNA-PK siRNA nearly completely depleted the ATM, ATR, and DNA-PK proteins. However, there was no significant difference in P3 foci formation after DNA damage between control and ATM, ATR, or DNA-PK knockdown cells, respectively. These data indicated that P3 foci can be constituted by more than one member of the PIKKs family. Additionally, because P3 is downstream target gene of p53, we also investigated whether P3 foci formation is dependent to p53. We observed that P3 foci was also formed in Neuro2A $p53^{-/-}$ cells transfected with P3 (Figure 3E) after DNA damage, indicating that P3 foci formation is independent of p53.

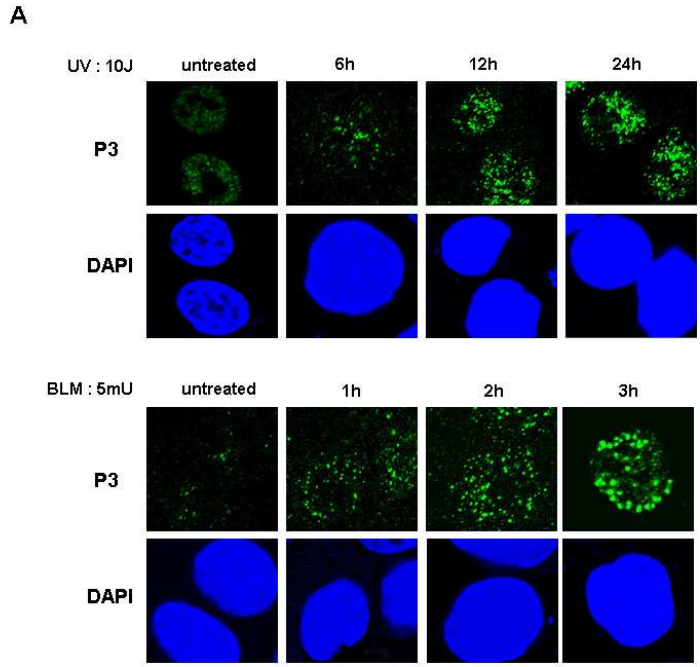

B

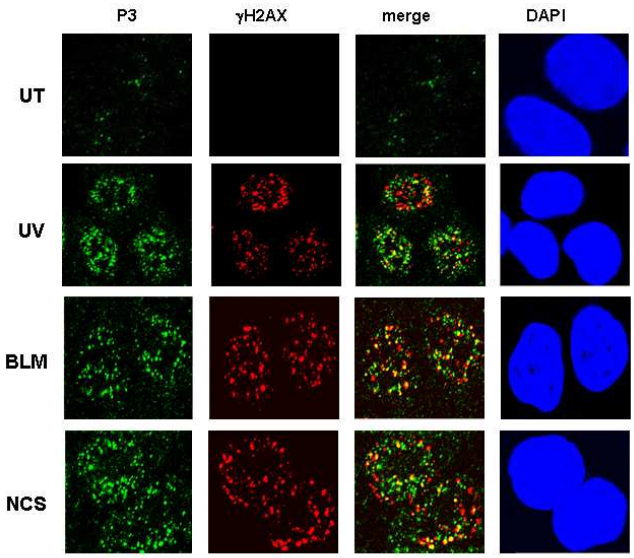
P3
γH2AX
merge
DAPI
UT
UV
BLM
NCS

C

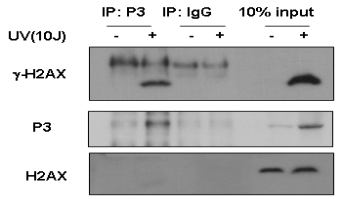
IP: P3
IP: IgG
10% input
UV(10J)
- + - + - +
γ-H2AX
P3
H2AX

D

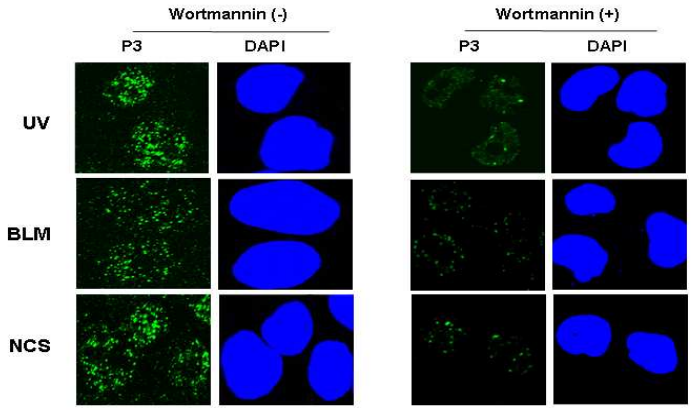
Wortmannin (-)
Wortmannin (+)
P3
DAPI
P3
DAPI
UV
BLM
NCS

E

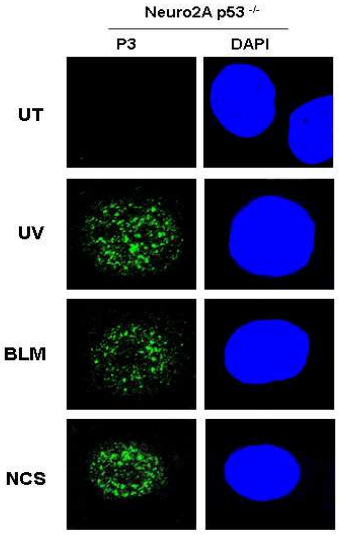
Neuro2A p53 -/-
P3
DAPI
UT
UV
BLM
NCS

Figure 3. P3 forms nuclear foci that colocalizes with γ-H2AX after DNA damages.

(A) Neuro2A cells were treated with UV(10 J/m^2) or BLM (5 mU) and immunostained with P3 antibody.

(B) Neuro2A cells were coimmunostained with anti-P3 and anti-γ-H2AX antibodies before and after treatment with UV (10 J/m^2), BLM (5 mU), or NCS (200 ng/ml).

(C) Unirradiated or UV (10 J/m^2)-irradiated Neuro2A cells were immunoprecipitated with P3 antibody and detected with indicated antibodeis.

(D) Neuro2A cells were pretreated with wortmannin prior to exposure to UV (10 J/m^2), BLM (5 mU), or NCS (200 ng/ml), and immunostained with P3 antibody.

(E) Neuro2A $p53^{-/-}$ cells were transiently transfected with control or P3 expression vectors. 48 hr after transfection, cells were treated with UV (10 J/m^2), BLM (5 mU), or NCS (200 ng/ml), and immunostained with P3 antibody.

5. Accumulation of 53BP1, Mre11, Rad50, Nbs1, and DNA-PK at the site of DNA damage foci is reduced in P3-depleted cells

Based on the current model, after DNA damage, γ-H2AX marks the chromatin region at or near the DNA damage site and serves as a platform for the recruitment of DNA damage response proteins including 53BP1, MDC1, MRN (Mre11-Rad50-Nbs1) complex, ATM, ATR, and DNA-PK. The appearance of these protein foci seems to be coincident with formation of the γ-H2AX. To further assess the possible role of P3 in the checkpoint signaling and its position within the signaling pathway, we determined whether P3 foci colocalizes with these proteins after DNA damage and whether P3 expression was required for the formation of foci containing these early response elements. We first analyzed foci formation using immunofluorescence staining with specific antibodies to P3, 53BP1, Mre11, Rad50, Nbs1, phospho-ATM (p-S1981), and DNA-PK. After UV, NCS, or BLM treatment, the numbers of P3 foci colocalized with 53BP1 (Figure 4A). Pig3 foci also colocalized with Mre11, Rad50, Nbs1, p-ATM, and DNA-PK foci following UV irradiation (Figure 4B). To confirm the colocalization between P3 and these proteins, we performed coimmunoprecipitation assay from HeLa total extracts. Immunoprecipitation with P3 antibody revealed that endogenous P3 bound 53BP1, component of MRN complex, ATM, ATR, and DNA-PK, and UV and NCS treatment increased the amount of P3 that bound to these proteins (Figure 4C). However, another DNA damage response proteins, BRCA1 and MDC1, were not associated with p3.

Because P3 colocalized and associated with several DNA damage sensors and mediators, we explored possible effects of P3 on localization of these proteins to DNA damage-induced foci. We observed that, following exposure of control HCT 116 cells to NCS (Figure 4D), UV and BLM, 53BP1, MRN complex, DNA-PK, ATM, and ATR

were readily recruited to DNA-damage sites. However, P3 knockdown cells exhibited a marked reduction in 53BP1, component of MRN complex, and DNA-PK foci formation. On the other hand, P3 depletion did not affect the ATM and ATR foci formation. In contrast to its effects on foci formation, pig3 knockdown did not change total levels of 53BP1, ATM, ATR, DNA-PK, Mre11, Nbs1 or Rad50. Thus, P3 is likely to function upstream of 53BP1, MRN complex, and DNA-PK, and contributes to the selective recruitment of these proteins into the sites of DNA break, leading to activation of DNA damage checkpoint pathway.

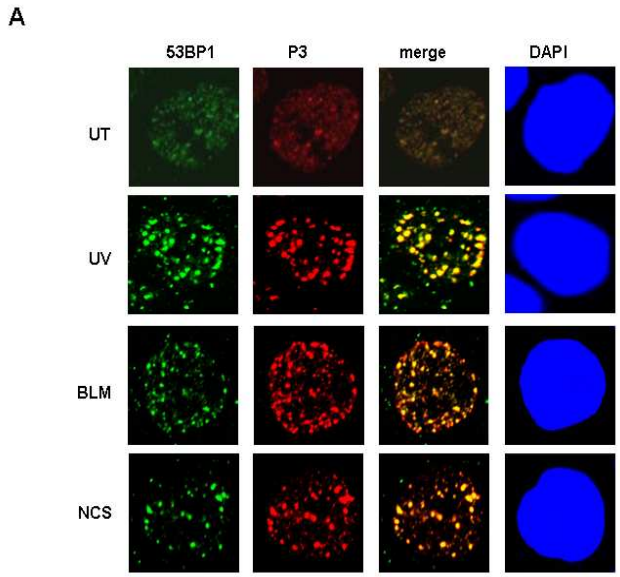

B

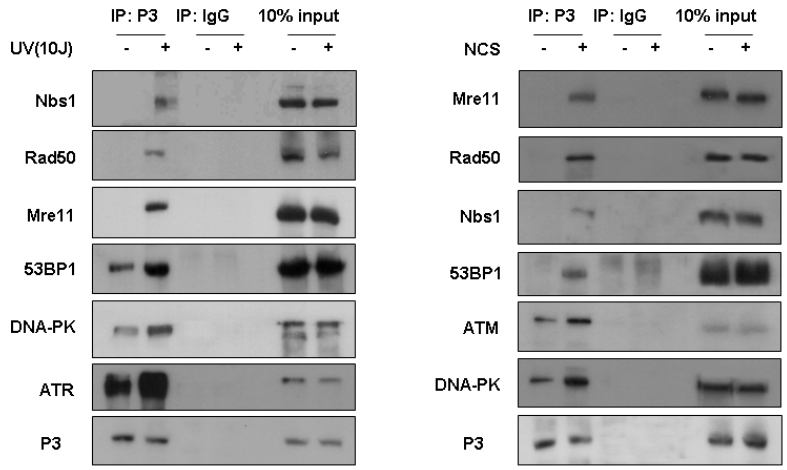
IP: P3
IP: IgG
10% input
UV(10J)
- + - + - +
Nbs1
Rad50
Mre11
53BP1
DNA-PK
ATR
P3
IP: P3
IP: IgG
10% input
NCS
- + - + - +
Mre11
Rad50
Nbs1
53BP1
ATM
DNA-PK
P3

C

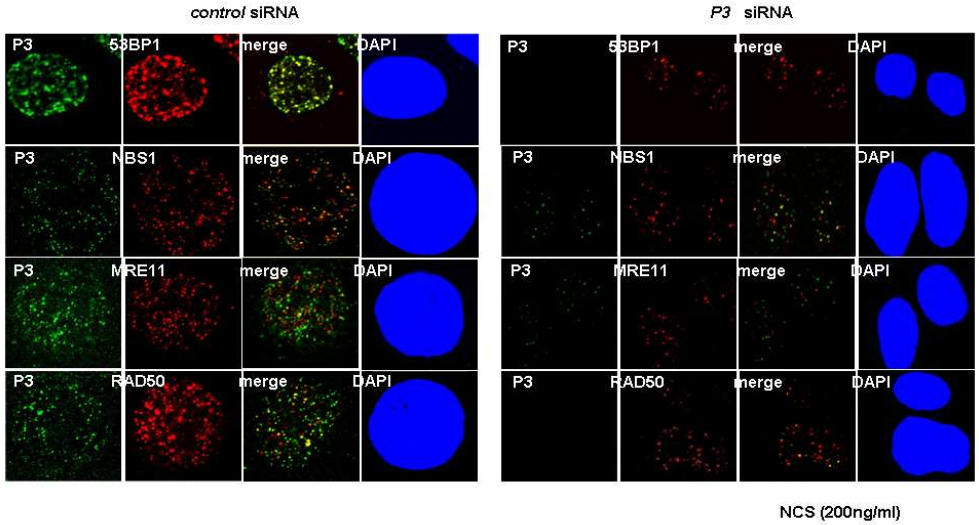
control siRNA
P3 siRNA
P3
53BP1
merge
DAPI
NBS1
MRE11
RAD50
NCS (200ng/ml)

D

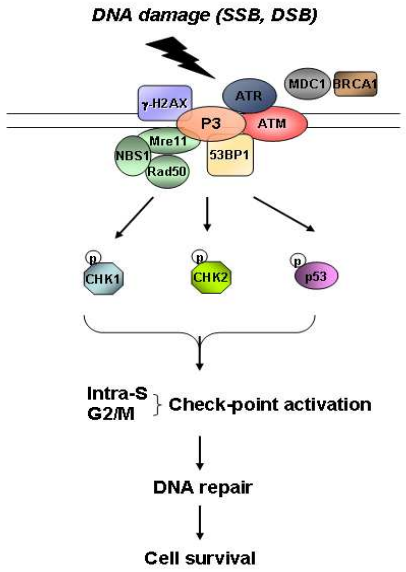
DNA damage (SSB, DSB)
γ-H2AX
ATR
MDC1
BRCA1
P3
ATM
Mre11
NBS1
Rad50
53BP1
P
CHK1
CHK2
p53
Intra-S
G2/M
Check-point activation
DNA repair
Cell survival

Figure 4. P3 is affecting the recruitment of the DNA damage sensors and mediators at the sites of DNA damage.

(A) Neuro2A cells were coimmunostained with anti-53BP1 and anti-P3 antibodies before and after treatment with UV (10 J/m^2), BLM (5 mU), or NCS (200 ng/ml).

(B) Neuro2A cells were untreated or treated with UV. 12 hr after treatment, cells were coimmunostained with indicated antibodies.

(C) Neuro2A cells were untreated or treated with UV (10 J/m^2) (left panel) and NCS (200 ng/ml) (right panel). Immunoprecipitation and immunoblotting were carried out using indicated antibodies.

(D) Control and P3-depleted Neuro2A cells were coimmunostained with indicated antibodies before and a 3 hr after treatment with NCS (200 ng/ml).

6. P3 is required for p53-mediated early DNA damage response

Although p53 is known to be a downstream effector of ATM/ATR signaling pathway, recent data also provide evidence for possible involvement of p53 in early DNA damage response. However, it is unclear whether p53 is indeed contributed to the early response to genotoxic stress, and if it is, how p53 functions to this process. To evaluate the ability of p53 to early cellular response to DNA damage, we treated p53 proficient and deficient cells with UV and BLM, and analyzed initial γ-H2AX signals. We observed that the degree of H2AX phosphorylation is distinctly lower in Neuro2A $p53^{-/-}$ (Figure 5A) and Saos-2 cells compared to Neuro2A and U2OS cells, respectively. Similarity, γ-H2AX foci formation after DNA damage was dramatically decreased in p53-deficient cells compared with p53-proficient cells.

Because P3 knockdown failed to efficient H2AX phosphorylation and γ-H2AX foci formation in p53 wild type cells following DNA damage (Figure 2), the reduction in P3 levels might cause decreased γ-H2AX signals in p53-deficient cells. To explore this possibility, we investigated whether P3 expression could be restored γ-H2AX signals in p53 deficient cells. Indeed, ectopic expression of P3 in Neuro2A $p53^{-/-}$ and Saos-2 cells almost completely restored both UV- and NCS-induced H2AX phosphorylation as well as γ-H2AX foci formation (Figure 5B and 5C).

To rule out the possibility that the impaired H2AX phosphorylation we observed is simply caused by a defect in p53 and subsequent suppression of DNA damage response, we compared the H2AX phosphorylation by UV in p53-proficient cells transiently transfected control siRNA or p53 siRNA. Importantly, downregulation of p53 for up to 48 hr did not cause any significant reduction of P3 levels. We found that transient transfection of p53 siRNA in Neuro2A and U2OS cells had no effect on H2AX phosphorylation following BLM treatment, indicating that the reduced DNA

damage-induced γ-H2AX signals cannot be ascribed simply to defect in p53 function. Instead, endogenous level of P3 may be sufficient for the activation of early cellular response to DNA damage.

To further address whether the suppression of early DNA damage response in p53 null cells was resulted from a downregulation of P3, we analyzed foci formation of 53BP1 and MRE11, which are early markers of DNA damage, in UV-, BLM-, and NCS-treated p53 null cells transfected with P3. We observed that, after UV, BLM, or NCS treatment, Neuro2A $p53^{-/-}$ and Saos-2 cells were severely suppressed foci formation of 53BP1 (Figure 5D) and MRE11 (Figure 5E) as compared those of Neuro2A $p53^{+/+}$ and U2OS cells, respectively. However, ectopically expressed P3 restored the 53BP1 and MRE11 foci formation in response to UV or NCS in Neuro2A $p53^{-/-}$ and Saos-2 cells. These results suggest that p53 functions to promote early response to DNA damage and P3 is required for these response.

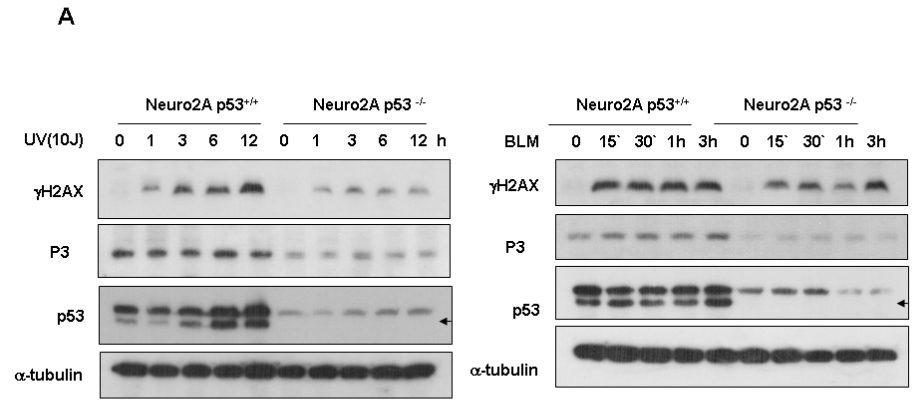
A
Neuro2A p53+/+
Neuro2A p53 -/-
UV(10J)
0 1 3 6 12 0 1 3 6 12 h
γH2AX
P3
p53
α-tubulin
Neuro2A p53+/+
Neuro2A p53 -/-
BLM
0 15` 30` 1h 3h 0 15` 30` 1h 3h
γH2AX
P3
p53
α-tubulin

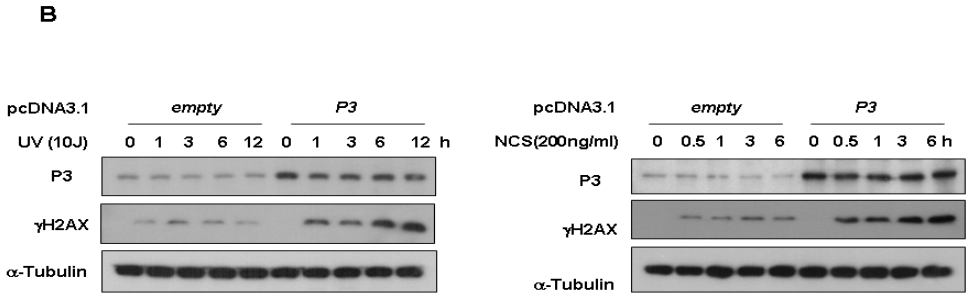
B
pcDNA3.1
empty
P3
UV (10J)
0 1 3 6 12 0 1 3 6 12 h
P3
γH2AX
α-Tubulin
pcDNA3.1
empty
P3
NCS(200ng/ml)
0 0.5 1 3 6 0 0.5 1 3 6 h
P3
γH2AX
α-Tubulin

C

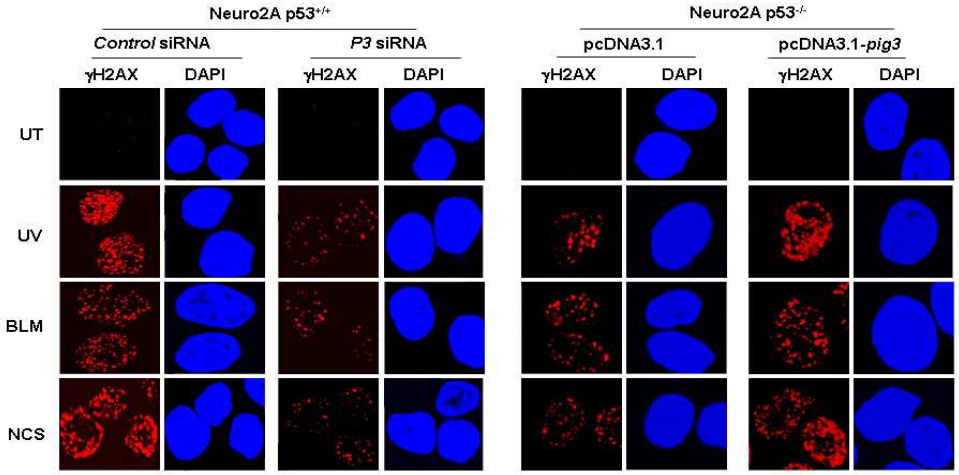
Neuro2A p53+/+
Control siRNA
P3 siRNA
Neuro2A p53-/-
pcDNA3.1
pcDNA3.1-pig3
γH2AX
DAPI
UT
UV
BLM
NCS

C

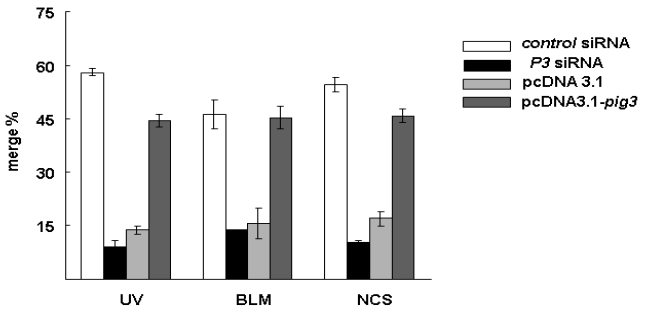
75
60
45
30
15
merge %
UV
BLM
NCS
control siRNA
P3 siRNA
pcDNA 3.1
pcDNA3.1-pig3

D

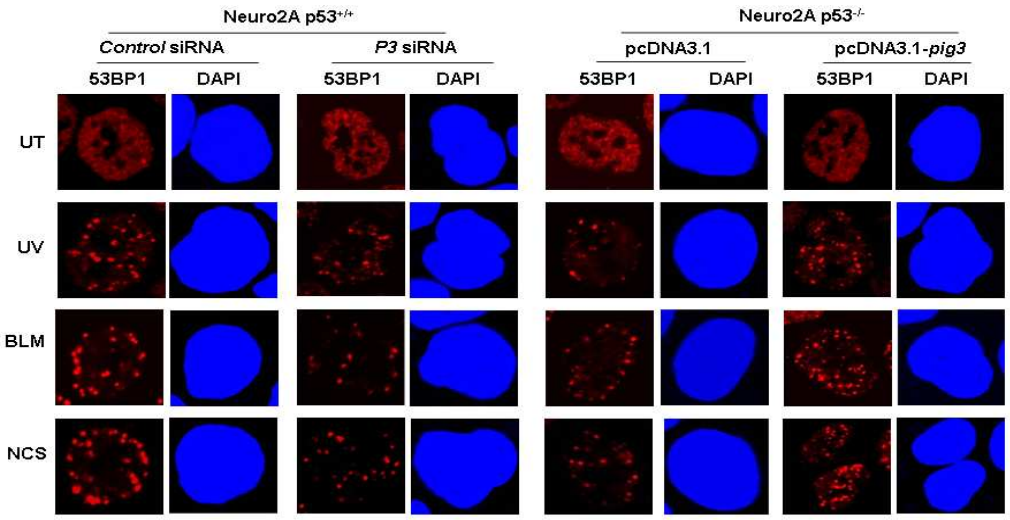
Neuro2A p53+/+
Control siRNA
P3 siRNA
53BP1
DAPI
53BP1
DAPI
Neuro2A p53-/-
pcDNA3.1
pcDNA3.1-pig3
53BP1
DAPI
53BP1
DAPI
UT
UV
BLM
NCS

D

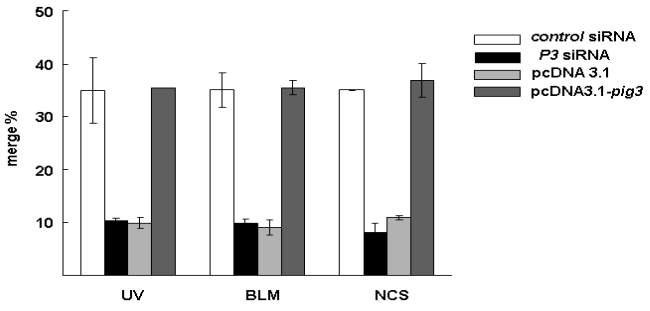
50
40
30
20
10
merge %
UV
BLM
NCS
control siRNA
P3 siRNA
pcDNA 3.1
pcDNA3.1-pig3

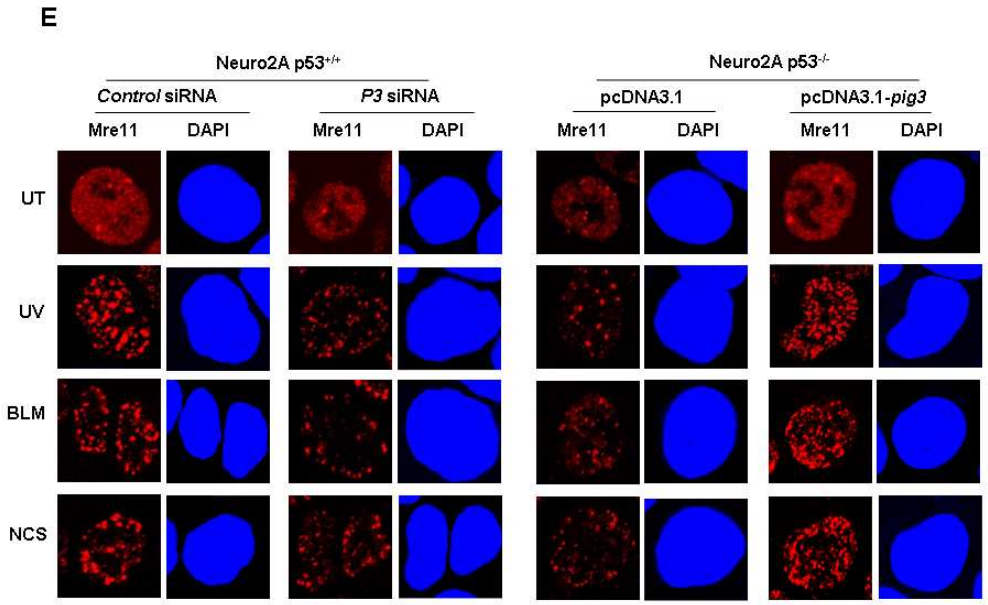
E
Neuro2A p53+/+
Neuro2A p53-/-
Control siRNA
P3 siRNA
pcDNA3.1
pcDNA3.1-pig3
Mre11
DAPI
UT
UV
BLM
NCS

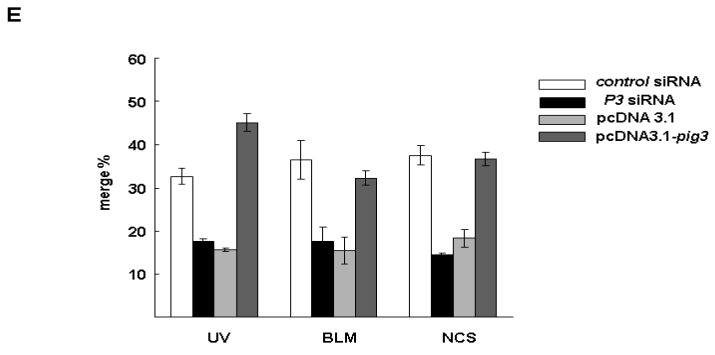
E
merge %
60
50
40
30
20
10
UV
BLM
NCS
control siRNA
P3 siRNA
pcDNA 3.1
pcDNA3.1-pig3

Figure 5. P3 is required for p53-mediated early DNA damage response.

(A) Neuro2A $p53^{+/+}$ and Neuro2A $p53^{-/-}$ cells were treated with 10 J/m^2 UV (left) and 5 mU BLM (right). At the indicated times after treatment, immunoblotting experiments were performed using indicated antibodies.

(B) Neuro2A $p53^{-/-}$ cells overexpressed of P3 were treated with 10 J/m^2 UV (left) or 200 ng/ml NCS (right), and immunoblotting experiments were performed using indicated antibodies.

(C-E) Neuro2A $p53^{+/+}$ cells depleted of endogenous P3 and Neuro2A $p53^{-/-}$ cells overexpressed of P3 were untreated or treated with UV (10 J/m^2), BLM (5 mU), or NCS (200 ng/ml), and immunostained with γ-H2AX (C), 53BPI (D), or Mre11 (E) antibodies. The percentage of cells with the respective foci are indicated. >100 cells were analyzed. Data are presented as mean ± standard deviation.

The number of nuclei positive for respective foci was measured in 100 cells for each transfectants.

DISCUSSION

The results presented in this study established p53 downstream target P3 as a novel and functional component in the DNA damage checkpoint signaling pathway, thereby expanding the scope of p53 targets to early DNA damage response (mediating DNA damage signaling). Our data strongly suggest that P3 contributes to the H2AX phosphorylation and foci formation at DNA damage sites to promote the accumulation of checkpoint proteins, such as 53BP1, MRN complex, ATM, and ATR. Moreover, we show that P3 contributes to the maintenance of the intra-S and G2/M checkpoint and its downregulation by shRNA accumulates DNA damage and confers increased sensitivity to DNA damaging reagents. We also found that this role of P3 in the DNA damage response is independent of p53 but is influenced by p53 mutation status.

P3 depletion impairs the upstream induction of DNA damage signals

Surprisingly, although P3 is know to be a p53-dependnet proapoptotic factor, P3 loss resulted in increased susceptibility to apoptotic cell death on exposure to UV radiation and radiomimetic drug. P3 knockdown Neuro2A and HeLa cells display increased susceptibility to apoptotic cell death on exposure to UV radiation and radiomimetic drug. The current study also shows that cells with P3 silencing showed a significantly reduction in DNA repair. Based on the CHEF and comet assay, we estimate 2- to 3-fold more unrepaired DNA damage in P3-deficient cells than control cells (Figure 1C and 1D). Moreover, P3 knockdown cells display a profound defect in the intra-S and G2/M checkpoint in response to UV or NCS. These observations may have been due to the impaired DNA damage response in P3 knockdown cells. Indeed, we show here that P3 to be an important sensor/mediator protein at the core of the DNA damage

response pathway, possibly involved in relaying the signal due to DNA damage to different effector pathways involved in DNA damage checkpoint and DNA repair. In fact, P3 foci rapidly accumulated at the sites of DNA strand breaks following UV, NCS, or BLM treatment, and P3 foci was formed by more than one members of PIKK family (Fig. 2B and Fig. S6). While P3 colocalizes with and associated with a variety of DNA damage checkpoint proteins such as γ-H2AX, 53BP1, MRN complex, ATM, and ATR, it also affects recruitment of 53BP1 and MRN complex to damaged DNA loci. Of interest is that P3 did not affect localization of MDC1 and BRCA1 to sites of DNA damage, suggesting that the latter are subject to a different regulation, somewhat similar to the parallel interacting pathways shown for 53BP1 and MDC1 in ATM activation (50). We also show that P3 depletion interfered with the formation of UV- and NCS-induced H2AX phosphorylation and γ-H2AX foci formation analyzed by Western blot analysis (Figure 2A and 2B) and fluorescent staining (Figure 2C and 2D), indicating P3 functions in parallel with or upstream of γ-H2AX in the signal pathways. Although we do not yet understand the function of P3 in the DSB-flanking chromatin compartment, one intriguing possibility is that P3-bound DNA damage sensor proteins accumulates on chromatin regions near DSBs, which leads to further spread of H2AX phosphorylation into more distal chromatin regions, thus helping to trigger a DNA damage response event even in the presence of very low number of DNA damage. Phosphorylation and relocalization of H2AX are two of the earliest events after DNA damage and are ATM/ATR-dependent. Thus, P3 might have a crucial role in early DNA damage responses in both ATM and ATR pathways. Although some crosstalk exists between ATM and ATR kinase pathways (51), ATM is activated primarily by DNA double-strand breaks (DDBs) induced by ionizing radiation, whereas ATR responds to ultraviolet (UV) radiation or stalled replication forks (11). Recent studies

also suggest the Mre11/Rad50/NBS1 (MRN) complex is responsible for the optimal activation and initial recruitment of ATM to DSBs (50, 52-58). This initial recruitment of ATM by MRN complex could result in the initial H2AX phosphorylation (6, 55, 59). Our current findings showed that P3 contributed to the recruitment of MRN complex, 53BP1 to damaged DNA loci, it may function as a key regulator in initiating the ATM/ATR-dependent response. In fact, P3 was unable to ATM and ATR autophosphorylation following DNA damage (data not shown). However, P3 preferentially affects ATM and/or ATR to phosphorylate its substrate Chk2, Chk1, p53, and H2AX, and the defect of Chk2 phosphorylation in P3-deficient cells also correlated with reduced degradation of Cdc25A, suggesting that P3 regulates ATM/ATR downstream of its activation. In addition, we provided evidence that P3 and phospho-ATM are co-localized at γ-H2AX foci after DNA damage, and we detected an interaction between P3, and ATM or ATR. Thus, P3 may amplify ATM/ATR activity through its involvement in the interaction of ATM/ATR or through regulation of some of DNA damage sensor proteins such as MRN complex and 53BP1 at γ-H2AX foci.

A number of DNA damage response proteins undergo regulated phosphorylation. Therefore, we sought to determine whether P3 is phosphorylated after DNA damage. There are two SQ/TQ phosphorylation motifs (threonine 116 and serine 174) in P3 (Figure S24A), which may be targets for PIKKs . We observed that, after UV or NCS treatment, mobility shift of P3 occurred in human fibroblast GM00637 cells (Figure S24B). UV- and NCS-induced supershift of P3 was due to phosphorylation because it was eliminated by treatment of P3 with protein phosphatase (Figure S25C). We also confirmed this using monoclonal anti-threonine antibody after immunoprecipitation of the protein with anti-P3 antibody (Figure S24C, S24D, and S24E). Thus, P3 is

hyperphosphorylated in response to DNA damage, but how this is controlled remains unclear. However, it is very difficult to obtain consistent phosphorylation (band shift) results with the P3 protein in Neuro2A and HeLa cells, thus it is believes that this protein is very sensitive to extraction procedure, or is very unstable depending on cell lines.

P3 is critical factor in the p53-mediated DNA damage response.

p53 is a major downstream effector of DNA-damage kinase pathways, as evidenced by reports demonstrating that activation of ATM/ATR-Chk1/Chk2 triggers p53 phosphorylation that leads to cell-cycle arrest and/or apoptosis. However, recent studies have shown that the function of p53 in DNA damage response is more complex than this model. DNA damage sensor/mediator MDC1 regulates p53-depedent DNA damage response through association with p53 (60). Additionally, gain-of-function p53 mutant (p53R248W and R273H) directly disrupt the recruitment of nuclear MRN complex to the site of DNA damage through physical interaction between p53 mutants and MRN complex, leading to impaired recruitment of ATM to the sites of DNA damage (48). Moreover, p53 downstream target DNA polymerase η contribute to the regulation of ATM and ATR activity after DNA damage (61). Thus, p53 may be involved in the initial phase of the DNA-damage response thorough its downstream targets and/or association with sensors/mediators, however, p53 plays a poorly understood, potential role in early DNA damage response, which appears distinct from its role in downstream effect of ATM/ATR signaling. Here we suggest that p53 downstream target P3 is a critical mediator of p53 functions in early response to DNA damage. In fact, not only does p53 null cells show significantly suppressed UV- or NCS-induced H2AX phosphorylation, but p53 depletion has also shown to

interfere with the formation of γ-H2AX, 53BP1, and MRE11 foci. Because of diverse function of p53, it is possible that multiple factors may be involved in this phenomenon. However, overexpression of P3 almost completely rescued the suppression of early DNA damage response imposed by p53 deficiency, and furthermore, the absence of P3 led to defect in the cellular responses to DNA damage in p53 proficient cells. Instead, knockdown of p53 alone dose not result in a interfere of this response, as γ-H2AX, 53BP1, and Mre11 that accumulate at DNA damage foci were not significantly affected by transiently transfected with p53 siRNA in p53 wild type cells. Thus, P3 is specifically required for the p53-mediated early DNA damage checkpoint activation. Interestingly, there was no significant different control SW480 cells and P3 expressed or P3 knockdown SW480 cells in H2AX phosphorylation as well as γ-H2AX and 53BP1 foci formation. Since gain-of-function p53 mutant blocks MRE11 function, these data suggest that P3 might function parallel or downstream of MRE11. Thus, although P3 plays a crucial role in transducing early DNA damage checkpoint response, P3 differently functions according to p53 mutation status on mediating DNA damage signaling pathway.

Previous studies have suggested that P3 is induced in response to excessive DNA damage in a p53-dependent manner (62, 63). Increased P3 expression modulates the levels of intracellular reactive oxygen species (ROS), leading to triggering apoptosis (27, 64-66). However, we discovered that knockdown of endogenous of P3 provoked a DNA damage-induced cell death, which was attributed to the defect of DNA damage response in P3-deficient cells. This effect was not associated with enhanced P3 levels because basal level of P3 in p53 proficient cells was enough to facilitates DNA damage response. Following DNA damage, the cells may decide to activate a survival system through cell cycle checkpoint and DNA repair or in the face of extensive or

irreparable damage, the cell may activate apoptotic cell death. Thus, our data can be explained in the context of the model in Figure 7. We propose that in p53 wild type cells, after DNA damage, P3 facilitates the DNA damage checkpoint signaling pathway that can efficiently repair DSBs, which might serve as a mechanism to activate a prosurvival activity of P3. However, high levels of P3 induced by prolong and/or excessive DNA damage may sensitize cells to DNA damage-induced apoptotic cell death, emphasizing the importance of proper modulation of P3 protein levels to ensure normal DNA damage checkpoint progression. On the other hands, p53 null cells fail to efficient induction of early DNA damage response, which might be attributed to the lack of the P3 function in DNA damage checkpoint, because the basal P3 levels were very low in these cells. DNA damage response is abnormal in gain-of-function p53 mutant SW480 cells, and P3 expression in these cells resulted in a hypersensitivity to UV radiation and radiomimetic drugs. Surprisingly, overexpression of P3 itself caused a induction of apoptotic cell death in these cells. This abnormality may be attributed to defect in pig function and the failure to execute an efficient DNA damage response, thereby allowing high levels of P3 to enhance the proapoptotic function of this protein. Since p53 and ATM/ATR are critical for maintaining genome stability, defect of P3 function in DNA damage checkpoint in both p53 null cells and p53 gain of function mutant cells may lead to chromosomal instability. Future studies of P3 will lead to a better understanding of its role in the DNA damage response as well as in the p53 pathway.

In conclusion, we have identified p53 target P3 as a new component of the DNA damage response and have established that this protein is crucial for cells to mount effective responses to DNA damaging reagents. Specifically, following UV, BLM, or NCS, P3 is activated by PIKKs and cooperated with DNA damage response proteins

to elicit the activation of ATM/ATR and thereby trigger cell cycle checkpoint and DNA repair events. Our studies provide a essential role of P3 in early events of DNA damage signaling pathway and revealed the physiological function of P3 in p53-mediated DNA damage checkpoint activation and maintaining chromosome stability.

REFERENCES

1. Bartek, J. and Lukas, J. DNA damage checkpoints: from initiation to recovery or adaptation. Curr Opin Cell Biol, *19:* 238-245, 2007.
2. Harper, J. W. and Elledge, S. J. The DNA damage response: ten years after. Mol Cell, *28:* 739-745, 2007.
3. O'Driscoll, M. and Jeggo, P. A. The role of double-strand break repair - insights from human genetics. Nat Rev Genet, *7:* 45-54, 2006.
4. Rouse, J. and Jackson, S. P. Interfaces between the detection, signaling, and repair of DNA damage. Science, *297:* 547-551, 2002.
5. Shiloh, Y. ATM and ATR: networking cellular responses to DNA damage. Curr Opin Genet Dev, *11:* 71-77, 2001.
6. Falck, J., Coates, J., and Jackson, S. P. Conserved modes of recruitment of ATM, ATR and DNA-PKcs to sites of DNA damage. Nature, *434:* 605-611, 2005.
7. Abraham, R. T. PI 3-kinase related kinases: 'big' players in stress-induced signaling pathways. DNA Repair (Amst), *3:* 883-887, 2004.
8. Khanna, K. K. and Jackson, S. P. DNA double-strand breaks: signaling, repair and the cancer connection. Nat Genet, *27:* 247-254, 2001.
9. Canman, C. E., Lim, D. S., Cimprich, K. A., Taya, Y., Tamai, K., Sakaguchi, K., Appella, E., Kastan, M. B., and Siliciano, J. D. Activation of the ATM kinase by ionizing radiation and phosphorylation of p53. Science, *281:* 1677-1679, 1998.
10. Kastan, M. B. and Bartek, J. Cell-cycle checkpoints and cancer. Nature, *432:* 316-323, 2004.
11. Zhou, B. B. and Elledge, S. J. The DNA damage response: putting checkpoints in perspective. Nature, *408:* 433-439, 2000.

12. Levine, A. J. p53, the cellular gatekeeper for growth and division. Cell, *88:* 323-331, 1997.

13. Vogelstein, B., Lane, D., and Levine, A. J. Surfing the p53 network. Nature, *408:* 307-310, 2000.

14. Ryan, K. M., Phillips, A. C., and Vousden, K. H. Regulation and function of the p53 tumor suppressor protein. Curr Opin Cell Biol, *13:* 332-337, 2001.

15. Prives, C. and Hall, P. A. The p53 pathway. J Pathol, *187:* 112-126, 1999.

16. Banin, S., Moyal, L., Shieh, S., Taya, Y., Anderson, C. W., Chessa, L., Smorodinsky, N. I., Prives, C., Reiss, Y., Shiloh, Y., and Ziv, Y. Enhanced phosphorylation of p53 by ATM in response to DNA damage. Science, *281:* 1674-1677, 1998.

17. Shieh, S. Y., Ahn, J., Tamai, K., Taya, Y., and Prives, C. The human homologs of checkpoint kinases Chk1 and Cds1 (Chk2) phosphorylate p53 at multiple DNA damage-inducible sites. Genes Dev, *14:* 289-300, 2000.

18. Hirao, A., Kong, Y. Y., Matsuoka, S., Wakeham, A., Ruland, J., Yoshida, H., Liu, D., Elledge, S. J., and Mak, T. W. DNA damage-induced activation of p53 by the checkpoint kinase Chk2. Science, *287:* 1824-1827, 2000.

19. Abraham, R. T. Cell cycle checkpoint signaling through the ATM and ATR kinases. Genes Dev, *15:* 2177-2196, 2001.

20. Bell, D. W., Varley, J. M., Szydlo, T. E., Kang, D. H., Wahrer, D. C., Shannon, K. E., Lubratovich, M., Verselis, S. J., Isselbacher, K. J., Fraumeni, J. F., Birch, J. M., Li, F. P., Garber, J. E., and Haber, D. A. Heterozygous germ line hCHK2 mutations in Li-Fraumeni syndrome. Science, *286:* 2528-2531, 1999.

21. Bartek, J. and Lukas, J. Mammalian G1- and S-phase checkpoints in response to DNA damage. Curr Opin Cell Biol, *13:* 738-747, 2001.

22. Taylor, W. R. and Stark, G. R. Regulation of the G2/M transition by p53. Oncogene,

20: 1803-1815, 2001.

23. Vousden, K. H. and Lu, X. Live or let die: the cell's response to p53. Nat Rev Cancer, *2:* 594-604, 2002.

24. Brugarolas, J., Chandrasekaran, C., Gordon, J. I., Beach, D., Jacks, T., and Hannon, G. J. Radiation-induced cell cycle arrest compromised by p21 deficiency. Nature, *377:* 552-557, 1995.

25. Deng, C., Zhang, P., Harper, J. W., Elledge, S. J., and Leder, P. Mice lacking p21CIP1/WAF1 undergo normal development, but are defective in G1 checkpoint control. Cell, *82:* 675-684, 1995.

26. Ihrie, R. A. and Attardi, L. D. Perp-etrating p53-dependent apoptosis. Cell Cycle, *3:* 267-269, 2004.

27. Polyak, K., Xia, Y., Zweier, J. L., Kinzler, K. W., and Vogelstein, B. A model for p53-induced apoptosis. Nature, *389:* 300-305, 1997.

28. Contente, A., Dittmer, A., Koch, M. C., Roth, J., and Dobbelstein, M. A polymorphic microsatellite that mediates induction of PIG3 by p53. Nat Genet, *30:* 315-320, 2002.

29. Tanaka, T., Ohkubo, S., Tatsuno, I., and Prives, C. hCAS/CSE1L associates with chromatin and regulates expression of select p53 target genes. Cell, *130:* 638-650, 2007.

30. Nicholls, C. D., Shields, M. A., Lee, P. W., Robbins, S. M., and Beattie, T. L. UV-dependent alternative splicing uncouples p53 activity and PIG3 gene function through rapid proteolytic degradation. J Biol Chem, *279:* 24171-24178, 2004.

31. Sancar, A., Lindsey-Boltz, L. A., Unsal-Kacmaz, K., and Linn, S. Molecular mechanisms of mammalian DNA repair and the DNA damage checkpoints. Annu Rev Biochem, *73:* 39-85, 2004.

32. Manke, I. A., Nguyen, A., Lim, D., Stewart, M. Q., Elia, A. E., and Yaffe, M. B.

MAPKAP kinase-2 is a cell cycle checkpoint kinase that regulates the G2/M transition and S phase progression in response to UV irradiation. Mol Cell, *17:* 37-48, 2005.

33. Reinhardt, H. C., Aslanian, A. S., Lees, J. A., and Yaffe, M. B. p53-deficient cells rely on ATM- and ATR-mediated checkpoint signaling through the p38MAPK/MK2 pathway for survival after DNA damage. Cancer Cell, *11:* 175-189, 2007.

34. Bulavin, D. V., Higashimoto, Y., Popoff, I. J., Gaarde, W. A., Basrur, V., Potapova, O., Appella, E., and Fornace, A. J., Jr. Initiation of a G2/M checkpoint after ultraviolet radiation requires p38 kinase. Nature, *411:* 102-107, 2001.

35. Celeste, A., Fernandez-Capetillo, O., Kruhlak, M. J., Pilch, D. R., Staudt, D. W., Lee, A., Bonner, R. F., Bonner, W. M., and Nussenzweig, A. Histone H2AX phosphorylation is dispensable for the initial recognition of DNA breaks. Nat Cell Biol, *5:* 675-679, 2003.

36. Fernandez-Capetillo, O., Lee, A., Nussenzweig, M., and Nussenzweig, A. H2AX: the histone guardian of the genome. DNA Repair (Amst), *3:* 959-967, 2004.

37. Motoyama, N. and Naka, K. DNA damage tumor suppressor genes and genomic instability. Curr Opin Genet Dev, *14:* 11-16, 2004.

38. Paull, T. T., Rogakou, E. P., Yamazaki, V., Kirchgessner, C. U., Gellert, M., and Bonner, W. M. A critical role for histone H2AX in recruitment of repair factors to nuclear foci after DNA damage. Curr Biol, *10:* 886-895, 2000.

39. Bassing, C. H. and Alt, F. W. H2AX may function as an anchor to hold broken chromosomal DNA ends in close proximity. Cell Cycle, *3:* 149-153, 2004.

40. Stewart, G. S., Wang, B., Bignell, C. R., Taylor, A. M., and Elledge, S. J. MDC1 is a mediator of the mammalian DNA damage checkpoint. Nature, *421:* 961-966, 2003.

41. Flatt, P. M., Polyak, K., Tang, L. J., Scatena, C. D., Westfall, M. D., Rubinstein, L. A.,

Yu, J., Kinzler, K. W., Vogelstein, B., Hill, D. E., and Pietenpol, J. A. p53-dependent expression of PIG3 during proliferation, genotoxic stress, and reversible growth arrest. Cancer Lett, *156:* 63-72, 2000.

42. Bakkenist, C. J. and Kastan, M. B. Initiating cellular stress responses. Cell, *118:* 9-17, 2004.

43. Efeyan, A. and Serrano, M. p53: guardian of the genome and policeman of the oncogenes. Cell Cycle, *6:* 1006-1010, 2007.

44. Hollstein, M., Sidransky, D., Vogelstein, B., and Harris, C. C. p53 mutations in human cancers. Science, *253:* 49-53, 1991.

45. Roemer, K. Mutant p53: gain-of-function oncoproteins and wild-type p53 inactivators. Biol Chem, *380:* 879-887, 1999.

46. Sigal, A. and Rotter, V. Oncogenic mutations of the p53 tumor suppressor: the demons of the guardian of the genome. Cancer Res, *60:* 6788-6793, 2000.

47. Song, H. and Xu, Y. Gain of function of p53 cancer mutants in disrupting critical DNA damage response pathways. Cell Cycle, *6:* 1570-1573, 2007.

48. Song, H., Hollstein, M., and Xu, Y. p53 gain-of-function cancer mutants induce genetic instability by inactivating ATM. Nat Cell Biol, *9:* 573-580, 2007.

49. Xu, Y. Induction of genetic instability by gain-of-function p53 cancer mutants. Oncogene, *27:* 3501-3507, 2008.

50. Mochan, T. A., Venere, M., DiTullio, R. A., Jr., and Halazonetis, T. D. 53BP1 and NFBD1/MDC1-Nbs1 function in parallel interacting pathways activating ataxia-telangiectasia mutated (ATM) in response to DNA damage. Cancer Res, *63:* 8586-8591, 2003.

51. Bartek, J. and Lukas, J. Chk1 and Chk2 kinases in checkpoint control and cancer. Cancer Cell, *3:* 421-429, 2003.

52. Spycher, C., Miller, E. S., Townsend, K., Pavic, L., Morrice, N. A., Janscak, P., Stewart, G. S., and Stucki, M. Constitutive phosphorylation of MDC1 physically links the MRE11-RAD50-NBS1 complex to damaged chromatin. J Cell Biol, *181:* 227-240, 2008.

53. Carson, C. T., Schwartz, R. A., Stracker, T. H., Lilley, C. E., Lee, D. V., and Weitzman, M. D. The Mre11 complex is required for ATM activation and the G2/M checkpoint. Embo J, *22:* 6610-6620, 2003.

54. Difilippantonio, S., Celeste, A., Fernandez-Capetillo, O., Chen, H. T., Reina San Martin, B., Van Laethem, F., Yang, Y. P., Petukhova, G. V., Eckhaus, M., Feigenbaum, L., Manova, K., Kruhlak, M., Camerini-Otero, R. D., Sharan, S., Nussenzweig, M., and Nussenzweig, A. Role of Nbs1 in the activation of the Atm kinase revealed in humanized mouse models. Nat Cell Biol, *7:* 675-685, 2005.

55. Lee, J. H. and Paull, T. T. ATM activation by DNA double-strand breaks through the Mre11-Rad50-Nbs1 complex. Science, *308:* 551-554, 2005.

56. Uziel, T., Lerenthal, Y., Moyal, L., Andegeko, Y., Mittelman, L., and Shiloh, Y. Requirement of the MRN complex for ATM activation by DNA damage. Embo J, *22:* 5612-5621, 2003.

57. Lukas, C., Melander, F., Stucki, M., Falck, J., Bekker-Jensen, S., Goldberg, M., Lerenthal, Y., Jackson, S. P., Bartek, J., and Lukas, J. Mdc1 couples DNA double-strand break recognition by Nbs1 with its H2AX-dependent chromatin retention. Embo J, *23:* 2674-2683, 2004.

58. Wu, L., Luo, K., Lou, Z., and Chen, J. MDC1 regulates intra-S-phase checkpoint by targeting NBS1 to DNA double-strand breaks. Proc Natl Acad Sci U S A, *105:* 11200-11205, 2008.

59. You, Z., Chahwan, C., Bailis, J., Hunter, T., and Russell, P. ATM activation and its

recruitment to damaged DNA require binding to the C terminus of Nbs1. Mol Cell Biol, *25:* 5363-5379, 2005.

60. Nakanishi, M., Ozaki, T., Yamamoto, H., Hanamoto, T., Kikuchi, H., Furuya, K., Asaka, M., Delia, D., and Nakagawara, A. NFBD1/MDC1 associates with p53 and regulates its function at the crossroad between cell survival and death in response to DNA damage. J Biol Chem, *282:* 22993-23004, 2007.

61. Liu, G. and Chen, X. DNA polymerase eta, the product of the xeroderma pigmentosum variant gene and a target of p53, modulates the DNA damage checkpoint and p53 activation. Mol Cell Biol, *26:* 1398-1413, 2006.

62. Yang, G., Zhang, G., Pittelkow, M. R., Ramoni, M., and Tsao, H. Expression profiling of UVB response in melanocytes identifies a set of p53-target genes. J Invest Dermatol, *126:* 2490-2506, 2006.

63. Long, X. H., Zhao, Z. Q., He, X. P., Wang, H. P., Xu, Q. Z., An, J., Bai, B., Sui, J. L., and Zhou, P. K. Dose-dependent expression changes of early response genes to ionizing radiation in human lymphoblastoid cells. Int J Mol Med, *19:* 607-615, 2007.

64. Asher, G., Lotem, J., Cohen, B., Sachs, L., and Shaul, Y. Regulation of p53 stability and p53-dependent apoptosis by NADH quinone oxidoreductase 1. Proc Natl Acad Sci U S A, *98:* 1188-1193, 2001.

65. Venot, C., Maratrat, M., Dureuil, C., Conseiller, E., Bracco, L., and Debussche, L. The requirement for the p53 proline-rich functional domain for mediation of apoptosis is correlated with specific PIG3 gene transactivation and with transcriptional repression. EMBO J, *17:* 4668-4679, 1998.

66. Ostrakhovitch, E. A. and Cherian, M. G. Role of p53 and reactive oxygen species in apoptotic response to copper and zinc in epithelial breast cancer cells. Apoptosis, *10:* 111-121, 2005.

<국문초록>

신경세포 DNA손상 보호작용을 지닌 P3 연구

김 승 곤

지도교수 : 김 학 렬

조선대학교 대학원 의학과

P3 는 게놈 보전과 DNA 수복에 관여하는 중요한 유전자다. 그렇지만, CAF-l 이 DNA 수복에 어떻게 관여하는지는 많이 연구되어지지 않았다. 본 연구에서는 DNA double strand breaks (DSBs) 수복에서 P3 p150 의 생물학적인 역할을 연구했다. P3 p150 은 DSBs 수복 반응에서 우선적으로 활성화 되어지는 ATM (ataxia telangiectasia mutated) 유전자와 직접 상호작용을 한다. 또한, P3 p150 은 DSBs 수복이 일어나는 곳에 보충되고, 동시에 ATM 과 함께 집중된다. RNA interference 를 통한 P3 p150 의 silencing 은 ATM 과 H2AX 의 인산화를 감소시켰고, foci 형성 또한 약간 감소시켰다. 그러나, 53BP1, MDC1, BRCA1, Chk2 and MRN complex 같은 DSBs 수복에 관여하는 DNA 수복 단백질의 보충에는 영향을 미치지 않았다. 또한, P3 p150 이 knockdown 된 세포에서 Chk2 의 인산화는 지연되었고 감소되었다. 그렇지만, BRCA1 과 p53 의 인산화는 증가되었다. DSBs 를 일으키는 물질인 Neocasinostatin (NCS)를 처치한 후에 DNA 가 손상된 세포는 G2/M 기에서 세포주기가 정지하였다. 이러한 결과는 DSBs 수복에서 P3 p150 이 ATM 신호전달 경로를 조절함으로써 세포주기 정지에

관여한다는 것을 나타낸다. 결론적으로, DNA double strand breaks 수복에서 P3 p150 은 G2/M 기 DNA checkpoint 를 조절하고 ATM 신호전달 경로를 통해서 DNA 수복에 관여할 것으로 사료된다.

저작물 이용 허락서

학 과	의학과	학 번	20067351	과 정	박사
성 명	한글 : 김 승 곤 한문 : 金 勝 坤 영문 : Kim Seung-Gon				
주 소	광주 광역시 동구 소태동 모아 미래로 아파트 105-405				
연락처	E-MAIL : goodidea1110@hanmail.net				
논문제목	한글: 신경세포 DNA손상 보호작용을 지닌 P3 연구				
	영문: The study of the P3 on the neuroprotective effect against DNA damage				

본인이 저작한 위의 저작물에 대하여 다음과 같은 조건아래 조선대학교가 저작물을 이용할 수 있도록 허락하고 동의합니다.

- 다 음 -

1. 저작물의 DB구축 및 인터넷을 포함한 정보통신망에의 공개를 위한 저작물의 복제, 기억장치에의 저장, 전송 등을 허락함.
2. 위의 목적을 위하여 필요한 범위 내에서의 편집과 형식상의 변경을 허락함. 다만, 저작물의 내용변경은 금지함.
3. 배포·전송된 저작물의 영리적 목적을 위한 복제, 저장, 전송 등은 금지함.
4. 저작물에 대한 이용기간은 5년으로 하고, 기간종료 3개월 이내에 별도의 의사표시가 없을 경우에는 저작물의 이용기간을 계속 연장함.
5. 해당 저작물의 저작권을 타인에게 양도하거나 출판을 허락을 하였을 경우에는 1개월 이내에 대학에 이를 통보함.
6. 조선대학교는 저작물 이용의 허락 이후 해당 저작물로 인하여 발생하는 타인에 의한 권리 침해에 대하여 일체의 법적 책임을 지지 않음.
7. 소속대학의 협정기관에 저작물의 제공 및 인터넷 등 정보통신망을 이용한 저작물의 전송·출력을 허락함.

동의여부 : 동의(0) 반대( )

2009년 2 월 일

저작자: 김 승 곤 (서명 또는 인)

조선대학교 총장 귀하